

151

Division of United Aircraft Corporation  
Stratford, Connecticut,  
Attn: Mr. Rep. B. Beisel,  
Engineering Manager

Engineering DEPT. LIBRARY  
Chance Vought Aircraft  
Stratford, Connecticut

Source of Acquisition  
CASI Acquired

NATIONAL ADVISORY COMMITTEE FOR AERONAUTICS

ACR Sept. 1942  
SP - 257

THIS DOCUMENT AND EACH AND EVERY  
PAGE HEREIN IS HEREBY RECLASSIFIED  
FROM CONFIDENTIAL TO CONFIDENTIAL  
AS PER LETTER DATED 12 Dec 1942

ADVANCE CONFIDENTIAL REPORT #257

WIND-TUNNEL DEVELOPMENT OF AILERONS FOR  
THE CURTISS XP-60 AIRPLANE

By F. M. Rogallo and John G. Lowry

Langley Memorial Aeronautical Laboratory  
Langley Field, Va.

CLASSIFIED DOCUMENT

This document contains classified information affecting  
the National Defense of the United States within the  
meaning of the Espionage Act, U.S. 50,31 and 32.  
It is the property of the  
**Unclassified - Notice Remarkred 4/17/09**

any member of the armed  
forces, information or  
to persons in the military and naval services of the  
United States, appropriate civilian officers and employees  
of the Federal Government who have a legitimate interest  
therein, and to United States citizens of known loyalty and  
disposition who of necessity must be informed thereof.

September 1942

NATIONAL ADVISORY COMMITTEE FOR AERONAUTICS

ADVANCE CONFIDENTIAL REPORT

WIND-TUNNEL DEVELOPMENT OF AILERONS FOR  
THE CURTISS XP-60 AIRPLANE

By F. M. Rogallo and John G. Lowry

SUMMARY

An investigation was made in the LMAL 7- by 10-foot tunnel of internally balanced, sealed ailerons for the Curtiss XP-60 airplane. Ailerons with tabs and with various amounts of balance were tested. Stick forces were estimated for several aileron arrangements including an arrangement recommended for the airplane. Flight tests of the recommended arrangement are discussed briefly in an appendix. The results of the wind-tunnel and flight tests indicate that the ailerons of large or fast airplanes may be satisfactorily balanced by the method developed.

INTRODUCTION

In connection with the development of ailerons for the Curtiss XP-60 airplane, tests were made in the NACA 7- by 10-foot tunnel of the left wing panel of the 0.36-scale model of the airplane. The tests were undertaken in order to determine what aileron modifications would be necessary on the original airplane in order to reduce the stick force to an acceptable value. For comparative purposes, tests were made of an aileron similar to the aileron of the original airplane. Comparable data on the characteristics of this aileron were available from unpublished tests of the complete model in the 19-foot pressure tunnel and from unpublished flight tests of the full-scale airplane. Modifications made on the aileron in the wind tunnel were such as could be made easily on the airplane. Tests were made with three different hinge-axis locations to determine the effect of varying the aileron chord and balance without varying the over-all dimensions of the aileron including balance. Tests were also made of one aileron extended to

the wing tip. Tab characteristics were determined on two of the aileron arrangements. Aileron-control characteristics for the XP-60 airplane equipped with several arrangements of the aileron extending to the wing tip were estimated from the test results and are presented in graphical form. One of these arrangements has since been flight tested. (See the appendix and reference 1.)

The tests reported herein were completed in November 1941 and the results were then submitted to the Materiel Division, Army Air Corps, in the form of a confidential memorandum report.

#### APPARATUS AND METHODS

The test set-up is shown schematically in figure 1 and in the photographs of figure 2. A semispan wing was suspended in the 7- by 10-foot tunnel (reference 2) with the root chord adjacent to one of the vertical walls of the tunnel, the tunnel wall thereby serving as a reflection plane. The flow over a semispan in this set-up is essentially the same as it would be over a complete wing in a 7- by 20-foot tunnel. Although a very small clearance was maintained between the root chord of the wing and the tunnel wall, no part of the wing was fastened to or in contact with the tunnel wall. Since the wing panel was suspended entirely from the regular balance frame, as shown in figure 1, all of the forces and moments acting upon it might be determined. Provision was made for changing the angle of attack while the tunnel was in operation.

The ailerons were deflected by means of a calibrated torque rod connecting the outboard end of the aileron with a crank outside the tunnel wall. The hinge moments were determined from the twist of the rod. (See figs. 1, 2(c), and 2(d).)

When the lift and drag of the wing were determined, the ailerons were locked in the neutral position. For aileron tests the angle of attack was maintained constant at each of several predetermined values of lift coefficient, while the aileron was deflected through its complete range. Rolling and yawing moments due to deflection of the aileron were computed as the difference between the respective moments of the semispan about the plane of symmetry with aileron neutral and with aileron deflected.

The models are shown in figures 2 and 3, and some of their geometric characteristics are given as follows:

Wing (complete):

Area, square feet . . . . .	35.69
Span, feet . . . . .	14.92
Aspect ratio . . . . .	6.23
Taper ratio . . . . .	3:1
Root section . . . . .	NACA 66,2-118
Tip section . . . . .	NACA 66,2x-116

Aileron:

Balance (percent)	Span (ft)	Root-mean-square chord (ft)
43.8	3.06	0.338
56.3	3.06	.312
68.8	3.06	.286
56.3 extended to wing tip	3.64	.293

Aileron tab (one aileron):

Aileron balance (percent)	Tab design- nation	Tab span (ft)	Tab chord (percent $c_a$ )
68.8	Full span	3.06	26
68.8	Outboard	1.53	26
56.3 ex- tended to tip	Outboard	1.85	26

The outboard portion of the wing panel was one of those tested on the complete model in the 19-foot pressure tunnel. The inboard portion of the wing panel was especially constructed for the tests in the 7- by 10-foot tunnel. The change in dihedral between the inboard and outboard portions of the wing panels of the complete model was not reproduced in the semispan model. (See fig. 3.) The ailerons tested had three different amounts of balance, as shown in figure 4. The balance, or overhang, was measured from the hinge line of the aileron to the center of the seal; the aileron chord was measured from the hinge line to the trailing edge of the aileron. The ailerons of 36.75-inch span, with each of the three amounts of balance, were tested on the wing with the turned-up tip. (See figs. 2(a), 2(b), and 3.) The aileron that extended to the wing tip was tested with the symmetrical wing tip. (See figs.

2(c), 2(d), and 3.) Tabs of 0.26 aileron chord were built into the trailing edges of the medium- and large-balance ailerons. The tab on the large-balance aileron was full span but was divided at the center of the aileron span to permit tests of the outboard portion only. The tab on the medium-balance aileron was used only in the tests of the aileron that extended to the wing tip. The tab was located outboard of the midspan point of the original aileron, as shown in figure 4.

All tests were made at a dynamic pressure of 16.37 pounds per square foot, which corresponds to a velocity of about 80 miles per hour and to a test Reynolds number of about 1,900,000, based on the mean aerodynamic chord of 31.32 inches. The corresponding effective Reynolds number was about 3,000,000 because of the turbulence factor of 1.6 for the 7- by 10-foot tunnel. The effects on hinge moment of the low scale, low velocity, and high turbulence of the test conditions relative to flight conditions were not determined or estimated.

## RESULTS AND DISCUSSION

### Coefficients and Corrections

The test results are presented in figures 5 to 15, and the aileron-control characteristics of the airplane equipped with the extended tip aileron, as computed from the test results, are presented in figure 16.

The symbols used in the presentation of results are:

$C_L$  lift coefficient ( $L/qS$ )

$\Delta C_{LW}$  increment of lift due to wing alone

$\Delta C_{LF}$  increment of lift due to flap ( $C_L = \Delta C_{LW} + \Delta C_{LF}$ )

$C_D$  uncorrected drag coefficient ( $D/qS$ )

$C_l'$  rolling-moment coefficient ( $L'/qbS$ )

$C_n'$  yawing-moment coefficient ( $N'/qbS$ )

$C_h$  aileron hinge-moment coefficient ( $H_a/qb_a \bar{c}_a^2$ )

- c wing chord
- $c_a$  aileron chord measured along airfoil chord line from hinge axis of aileron to trailing edge of aileron
- $\bar{c}_a$  root-mean-square chord of aileron
- b twice span of semispan model
- $b_a$  aileron span
- S twice area of semispan model
- L twice lift on semispan model
- D twice drag on semispan model
- $L'$  rolling moment, due to aileron deflection, about wind axis in plane of symmetry
- V velocity, feet per second
- $N'$  yawing moment, due to aileron deflection, about wind axis in plane of symmetry
- $H_a$  aileron hinge moment
- q dynamic pressure of air stream  $(\frac{1}{2} \rho V^2)$  uncorrected for blocking
- $\alpha$  angle of attack
- $\delta_a$  aileron deflection relative to wing, positive when trailing edge is down
- $\delta_t$  tab deflection relative to aileron, positive when trailing edge is down
- $\delta_f$  flap deflection relative to wing, positive when trailing edge is down
- $C_{l_p}$  rate of change of rolling-moment coefficient  $C_l$  with helix angle  $p b / 2V$
- p rate of roll
- $F_s$  stick force

$T_s$  stick travel

A positive value of  $L'$  or  $C_l'$  corresponds to an increase in lift of the model, and a positive value of  $N'$  or  $C_n'$  corresponds to a decrease in drag of the model. Twice the actual lift, drag, area, and span of the model were used in the reduction of the results because the model represented half of a complete wing. The drag coefficient and the angle of attack have been corrected in accordance with the theory of trailing-vortex images. Corresponding corrections for the rolling- and yawing-moment coefficients, which have been derived but not applied, are

$$\Delta C_l' = -0.1 C_l'$$

$$\Delta C_n' = -(0.031 \Delta C_{LW} C_l' + 0.019 \Delta C_{LF} C_l' + 0.169 C_l'^2)$$

These corrections may be added to the uncorrected coefficients. No corrections have been applied to the hinge-moment coefficients and no corrections have been applied to any of the results for the effects of the support strut or the treatment of the inboard end of the wing; that is, for the small gap between the wing and the wall, the leakage through the wall around the support tube, and the boundary layer at the wall. A blanket correction for the rolling velocities to correct for differences between the wind-tunnel conditions and flight will be discussed later.

#### Lift and Drag

Lift and drag coefficients of the wing with and without a partial-span split flap are given in figure 5. These data were obtained with the aileron torque rod removed and the aileron locked in the neutral position. The flap-neutral curves were obtained with the arrangement incorporating the short-balance aileron and turned-up wing tip; whereas the flap-deflected curves were obtained after the installation of the symmetrical wing tip and aileron extending to the tip. The slopes of the lift curves of figure 5 are about 7 percent less than the corresponding slopes obtained in the 19-foot pressure tunnel at about the same Reynolds number, probably because of differences in the two set-ups. The maximum lift coefficients, however, are in fair agreement.

### Aileron with $0.438c_a$ Balance

The characteristics of the aileron with  $0.438c_a$  balance are presented in figures 6 to 8. Comparison of uncorrected data from the 7- by 10-foot tunnel with that from the 19-foot pressure tunnel (fig. 6) shows fair agreement. The results of the 19-foot pressure tunnel tests were corrected for model asymmetry in this figure. The aileron balance was not sealed at the ends of the aileron in either tunnel when the data of figure 6 were obtained. The effect of leaks on the rolling- and hinge-moment coefficients is shown in figure 7, and the data of figure 8 were obtained with the balance sealed along the entire span and at the ends. The data of figure 8 are thought to be comparable with the unpublished flight-test results.

### Aileron with $0.563c_a$ Balance

The characteristics of the aileron with  $0.563c_a$  balance ( $b_a = 36.75$  in.) are presented in figure 9. Comparison of these results with those of figure 8 shows that the hinge-moment coefficients have been greatly reduced and, as would be expected, there has been a small loss in rolling-moment coefficient due to the reduction of aileron chord.

### Aileron with $0.688c_a$ Balance

The aileron with  $0.688c_a$  balance was tested through a wide range of angles of attack with the tab neutral (fig. 10) and tests were also made at two lift coefficients with a full-aileron-span tab deflected various amounts (fig. 11). Two tests were made with only the outboard half of the tab deflected (fig. 12).

The results indicate that a considerable increase in rolling-moment coefficient may be obtained by moving the hinge axis back to a position of overbalance and then deflecting the tab to provide unbalance.

### Variation of $\delta C_h/\delta \alpha$ and $\delta C_h/\delta \delta_a$ with Aileron Balance

The effect of balance variation upon the slopes of the hinge-moment-coefficient curves,  $\delta C_h/\delta \delta_a$  and

$\delta C_h/\delta \alpha$ , are shown in figure 13. The values of  $\delta C_h/\delta \delta_a$  were computed from the test points at  $\delta_a$  of  $5^\circ$  and  $-5^\circ$  at  $\alpha = 0$ ; slightly different values would have been obtained if a different range or angle of attack had been considered. The values of  $\delta C_h/\delta \alpha$  were computed from test results at  $\alpha$  of approximately  $0^\circ$  and  $10^\circ$  for  $\delta_a = 0^\circ$ . Although the trend of  $\delta C_h/\delta \delta_a$  is about as was expected, the variation of  $\delta C_h/\delta \alpha$  with balance is much less than was expected, probably because the hinge location was varied as well as the percent balance. It is thought that if the aileron chord had been maintained constant and only the balance had been varied, the numerical magnitude of  $\delta C_h/\delta \alpha$  would have decreased more rapidly with increasing balance than is shown in figure 13.

The points for 20 percent balance (fig. 13) were obtained from tests of the 43.8-percent-balance aileron with seal completely removed. It was reasoned that, with the seal completely removed, there would be no pressure difference between the upper and lower surfaces of the aileron nose. The nose would, therefore, contribute no hinge moment and the hinge-moment characteristics would be the same as if the aileron had a semicircular nose, sealed or unsealed. A semicircular nose would have an overhang or balance of about half the airfoil thickness at the hinge (for this particular aileron,  $0.20c_a$ ). By this line of reasoning it follows that an internally balanced aileron with a large unsealed clearance at its nose will have the same hinge-moment characteristics regardless of its overhang and that an aileron with a nose overhang of less than half the airfoil thickness at the hinge, if sealed, will provide negative balance relative to a semicircular nose.

It is evident from this discussion, which is supported by unpublished test results, that, as the thickness of airfoils is increased near the trailing edge, the amount of balance or overhang of the control surface must also be increased if the same balancing action is to be maintained. It is also evident that the effectiveness of an internal balance is very dependent upon the amount of leakage past the seal. In many applications it may be found convenient to adjust the stick-force characteristics by changing the leakage area as, for example, by the insertion of grommets in the seal. Some leakage, moreover, will probably be necessary to permit drainage of water. The effect of removal of the seal upon the rolling-moment coefficient of

the small-balance aileron is shown to be appreciable in figure 7. These data also show that for small leakage the loss in rolling-moment coefficient is small.

#### Aileron with Extended Tip

The characteristics of the aileron extended to the wing tip with 0.563 $c_a$  balance are presented in figures 14 and 15. Results for the tab neutral condition at several lift coefficients are given in figure 14. The effect of tab deflection is shown in figure 15.

Comparison of figure 14 with figure 8 shows that the aileron with extended tip gave a greater rolling-moment coefficient per degree of aileron deflection than did the aileron of greater chord but shorter span.

#### Computation of Aileron-Control Characteristics for the Airplane

Aileron-control characteristics for the airplane computed from figures 14 and 15 are presented in figure 16. In the computations the following characteristics were assumed:

$$w/S = 33.68 \text{ pounds per square foot}$$

$$C_{l_p} = 0.55$$

Maximum stick travel,  $\pm 7.5$  inches

Maximum aileron deflection,  $\pm 14^\circ$

The hinge-moment and rolling-moment coefficients used in the computations were obtained from cross plots of the aileron characteristics against angle of attack, and account was taken of the effect of change in angle of attack over the aileron portion of the wing due to rolling velocity. For the calculations a straight line variation of aileron deflection with stick travel was assumed.

The value of  $C_{l_p} = 0.55$  was computed from the rates of roll of the airplane in flight and the values of  $C_l'$

from wind-tunnel tests of the aileron with  $0.438c_a$  balance (fig. 8). This aileron was similar to the ailerons on the airplane. That is,

$$C_{l_p} = \frac{C_l' \text{ (from wind tunnel)}}{pb/2V \text{ (from flight)}}$$

Although the damping coefficient  $C_{l_p}$  decreases near the stall, the value of 0.55, which is the average of determinations at lift coefficients of 0.30 and 0.46, was used in the computations of all the characteristics of figure 16. The use of an adjusted damping coefficient in the computation of rates of roll from wind-tunnel data is thought to correct for differences between the wind-tunnel and flight conditions.

The ailerons without tabs are slightly overbalanced at low deflections because of the high value of  $\partial C_h / \partial \alpha$  relative to  $\partial C_h / \partial \delta_a$ . It is probable that, by use of a spring to obtain proper aileron feel, such an arrangement would be satisfactory. The hinge-moment coefficient of each aileron, it must be remembered, is that corresponding to the local angle of attack at the aileron during roll at  $pb/2V$  of  $C_l'/C_{l_p}$ , where  $C_l'$  is the uncorrected rolling-moment coefficient from wind-tunnel results (fig. 14) and  $C_{l_p}$  is the adjusted damping coefficient.

In order to make the system stable in all flight conditions, an unbalancing tab deflection of  $\delta_t/\delta_a = 1$  was assumed. (See fig. 16(b).) From these results it appeared that the maximum stick forces might be reduced somewhat without overbalancing in any condition if a smaller tab or a lower tab deflection was used.

Because the Curtiss-Wright Corporation preferred to reduce the span rather than the deflection, a  $0.26c_a$  tab of one-third the span of the original aileron ( $b_a = 36.75$  in. on the model) was assumed. (See fig. 17.) It was estimated from the data of figures 11 and 12 that the assumed tab would be half as effective as the tested tab. The computed rolling characteristics of the airplane equipped with this assumed tab linked for  $\delta_t/\delta_a = 1$  are given in figure 16(c).

In figure 16(d) are presented estimated characteristics for the airplane equipped with the aileron assumed in the computations of figure 16(c), but with the overhang or balance increased to 0.60 $c_a$ . (See fig. 17.) There was no change of aileron size, tab size, or linkages. It was estimated from figure 13 that the effect of the increase in balance was to increase, in the direction of overbalance, the value of  $\partial C_h / \partial \delta_a$  by 0.0009. A curve of the stick force that would be experienced if the aileron could be deflected without the airplane's rolling is shown on figure 16(d) for comparison.

#### RECOMMENDATIONS

It is recommended that the ailerons of the XP-60 airplane be made similar to the ailerons assumed in the computation of figure 16(d). (See fig. 17.) If the ailerons are found to be overbalanced, an increase in area of leakage past the seal may be made by the insertion of grommets or by provision of clearance at the ends of the aileron. If the stick forces are too high, the ratio of tab to aileron motion may be reduced. In the initial design, however, it is recommended that the seal be made as effective as possible.

Because of the low aerodynamic stick forces of the arrangement, great care should be taken to eliminate unnecessary friction in the aileron-control linkage.

Langley Memorial Aeronautical Laboratory,  
National Advisory Committee for Aeronautics,  
Langley Field, Va.

#### APPENDIX

Flight tests on the XP-60 airplane have been made of an aileron arrangement similar to that recommended in the present report. (See reference 1.) The linked tab was found unnecessary and was locked in position. With the locked tab, the stick force at an indicated airspeed of

268 miles per hour with a total aileron deflection of 28° was 37 pounds, which was considerably greater than would have been estimated for those conditions. The discrepancy could have been due to the difference in scale, velocity, or turbulence, or to differences in the details of construction. The large effect of leakage on the hinge-moment has been shown in the present report. More recent wind-tunnel tests have indicated that the alignment of the balance cover plates also has a large effect upon the hinge-moment characteristics.

Pilots have been very favorably impressed by the characteristics of the XP-60 ailerons, and the results of the flight tests were summarized in reference 1 as follows:

"The results show that light and effective aileron control was obtained without evidence of overbalance or undesirable shaking of the control system at any part of the deflection range within the level-flight speed range."

#### REFERENCES

1. Gilruth, R. R.: Flight Tests of Internally Balanced, Sealed Ailerons on the Curtiss XP-60 Airplane. NACA C.B., July 1942.
2. Wenzinger, Carl J., and Harris, Thomas A.: Wind-Tunnel Investigation of an N.A.C.A. 23012 Airfoil with Various Arrangements of Slotted Flaps. Rep. No. 664, NACA, 1939.

NACA

Fig. 1

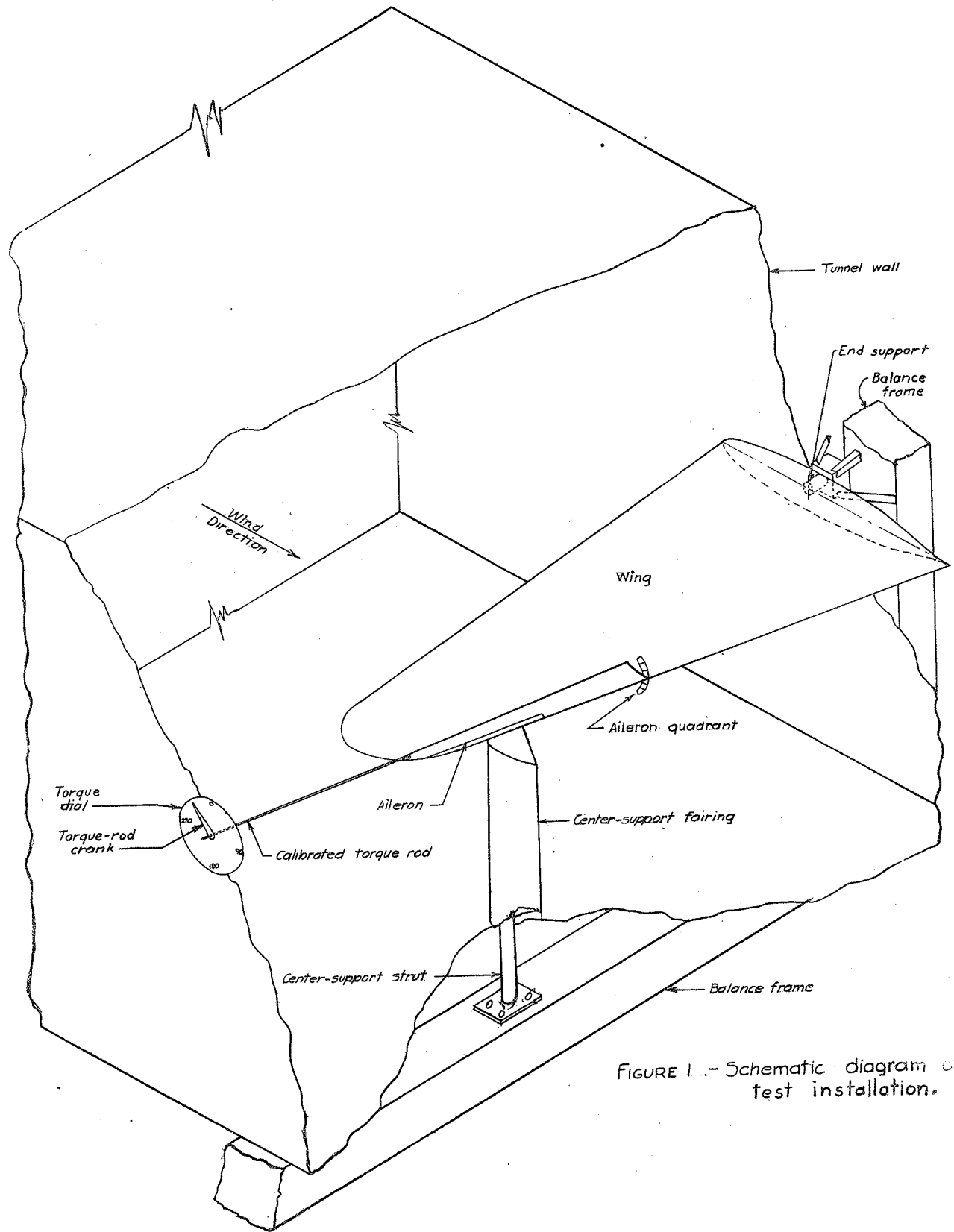
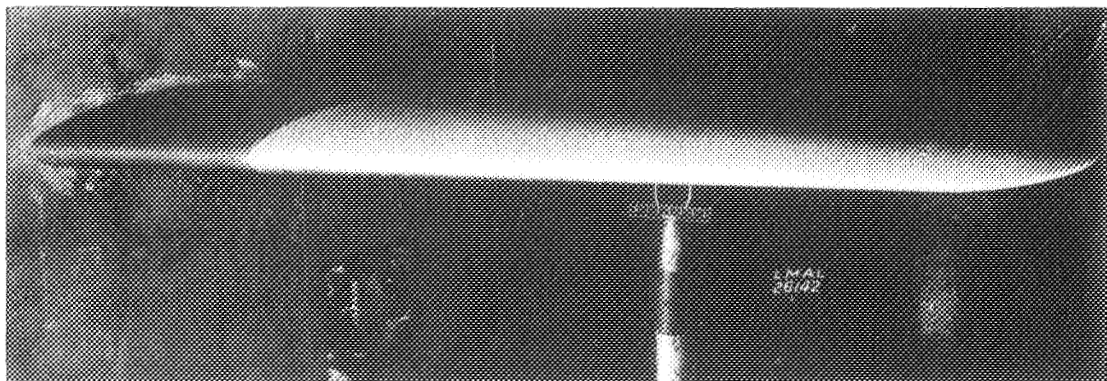
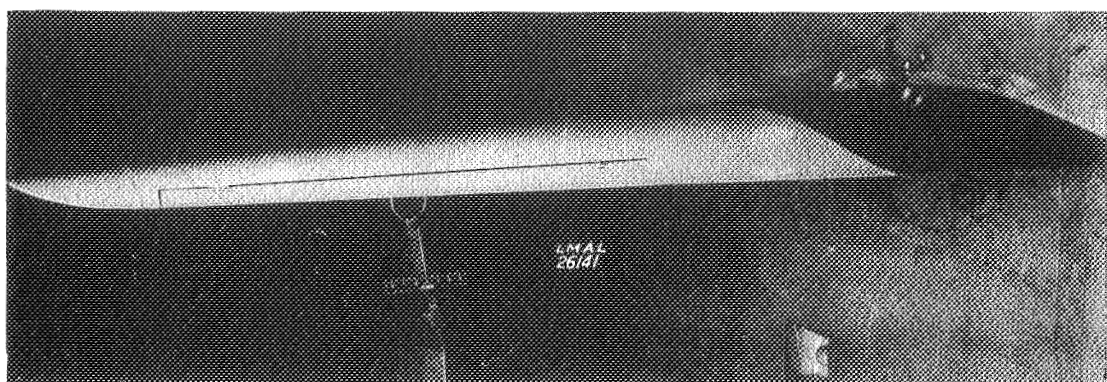


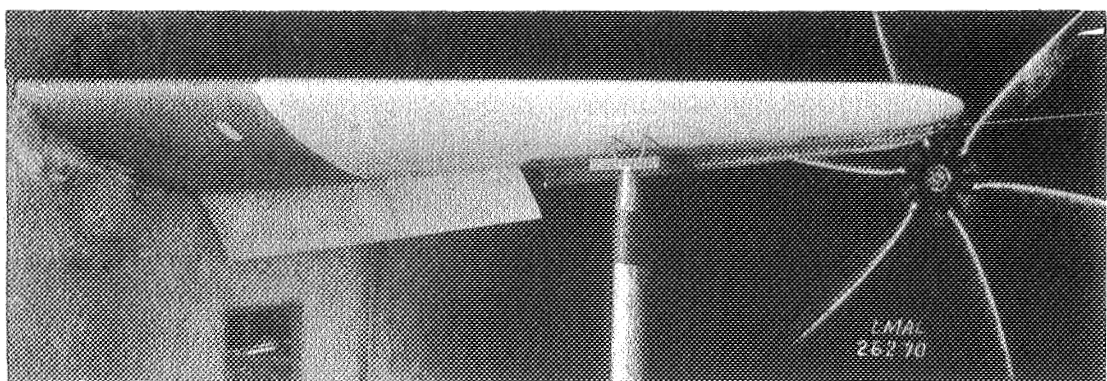
FIGURE 1.—Schematic diagram of  
test installation.



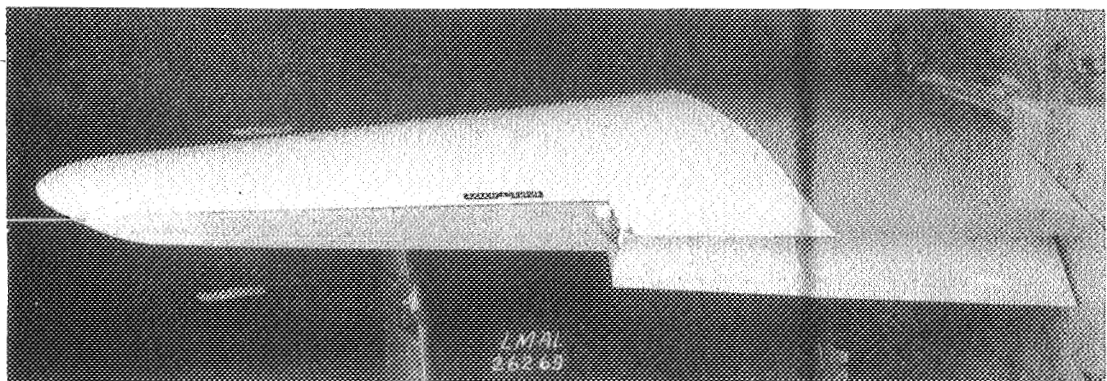
(a) Three-quarter front view; flap removed; turned-up tip.



(b) Three-quarter rear view; flap removed; turned-up tip.



(c) Three-quarter front view; flap, 45°; symmetrical tip.



(d) Three-quarter rear view; flap, 45°; symmetrical tip.

Figure 2a to d.- Semispan of the 0.36-scale model of the Curtiss XP-60 wing in the  
7- by 10-foot wind tunnel.

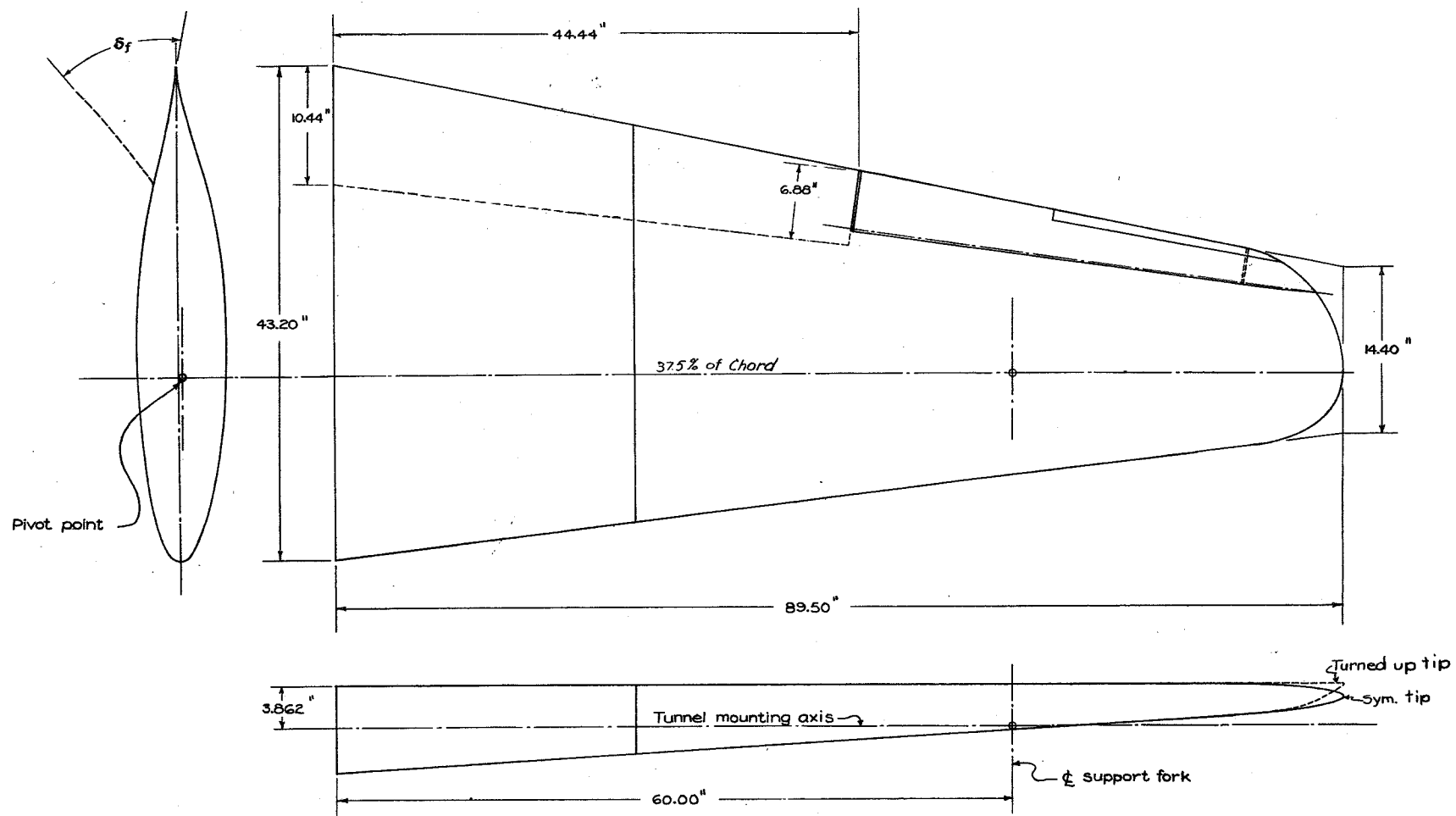


FIGURE 3.— Semispan wing of 0.36-scale model of Curtiss XP-60 airplane as tested in NACA 7- by 10-foot wind tunnel.

NACA

Figs. 4,17

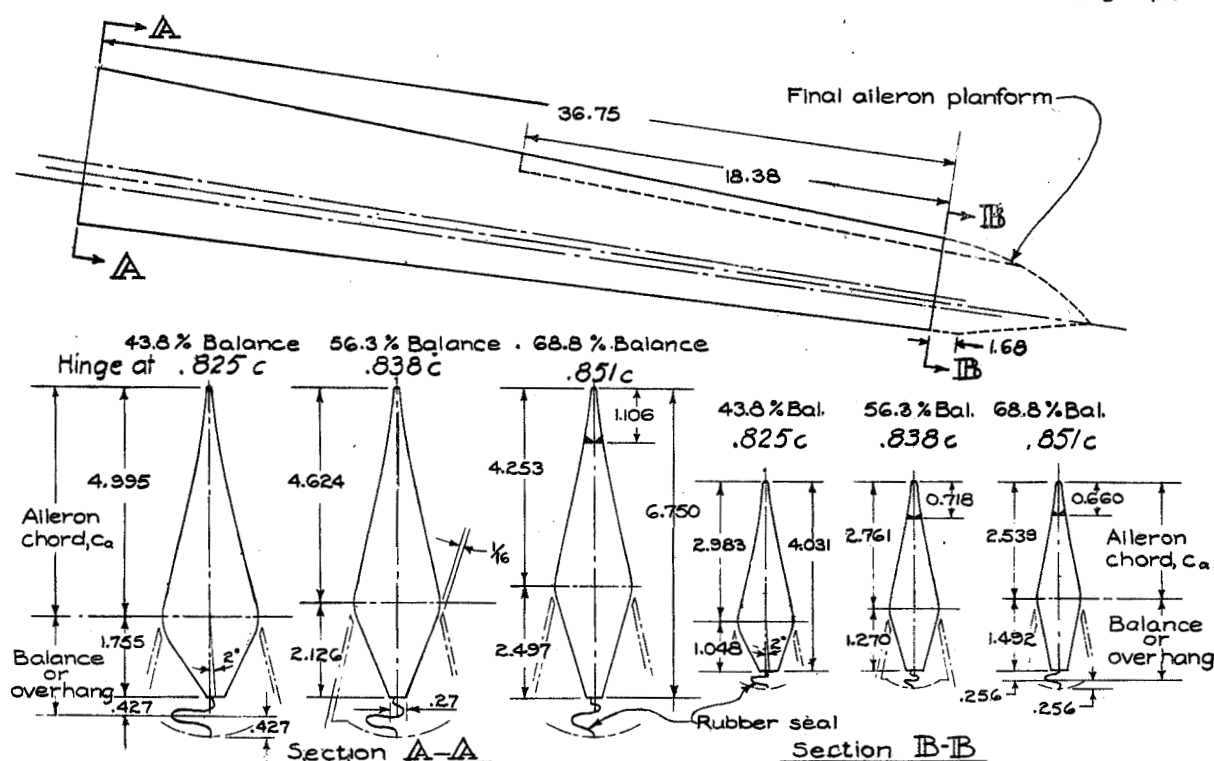


FIGURE 4.- Ailerons of 0.36-scale wing model of Curtiss XP-60 airplane as tested in the NACA 7- by 10-foot wind tunnel.

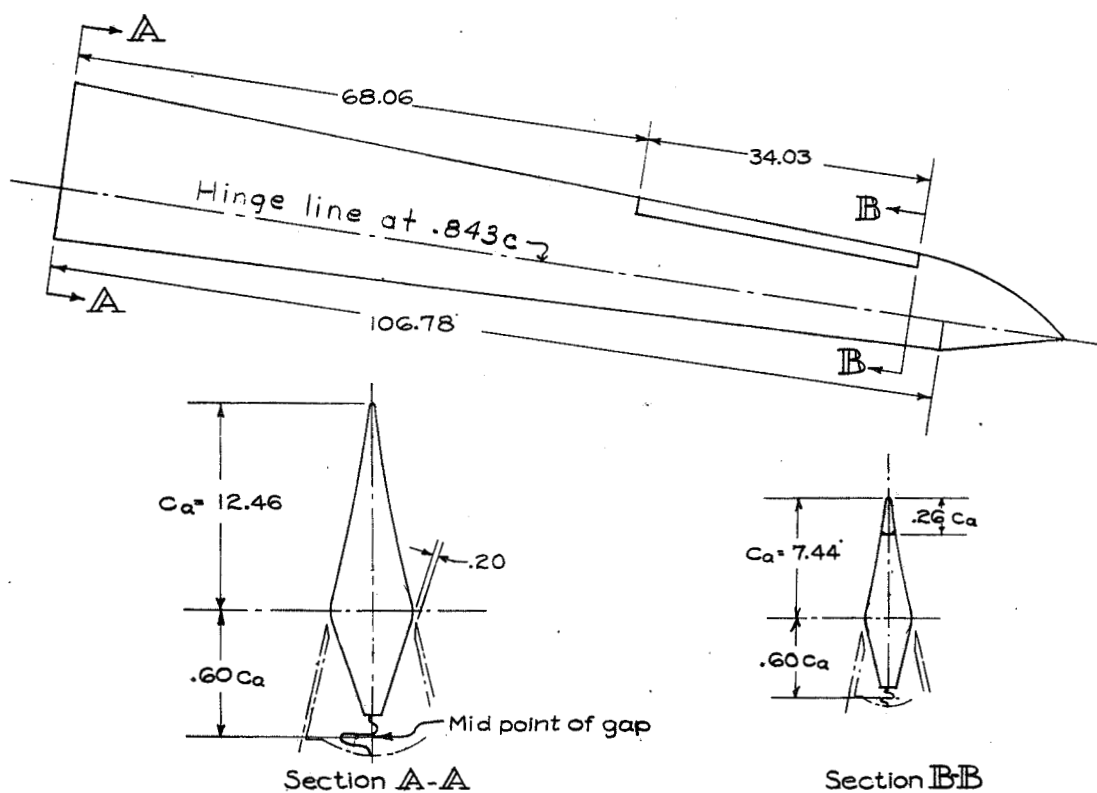


FIGURE 17.- Recommended aileron for Curtiss XP-60 airplane.

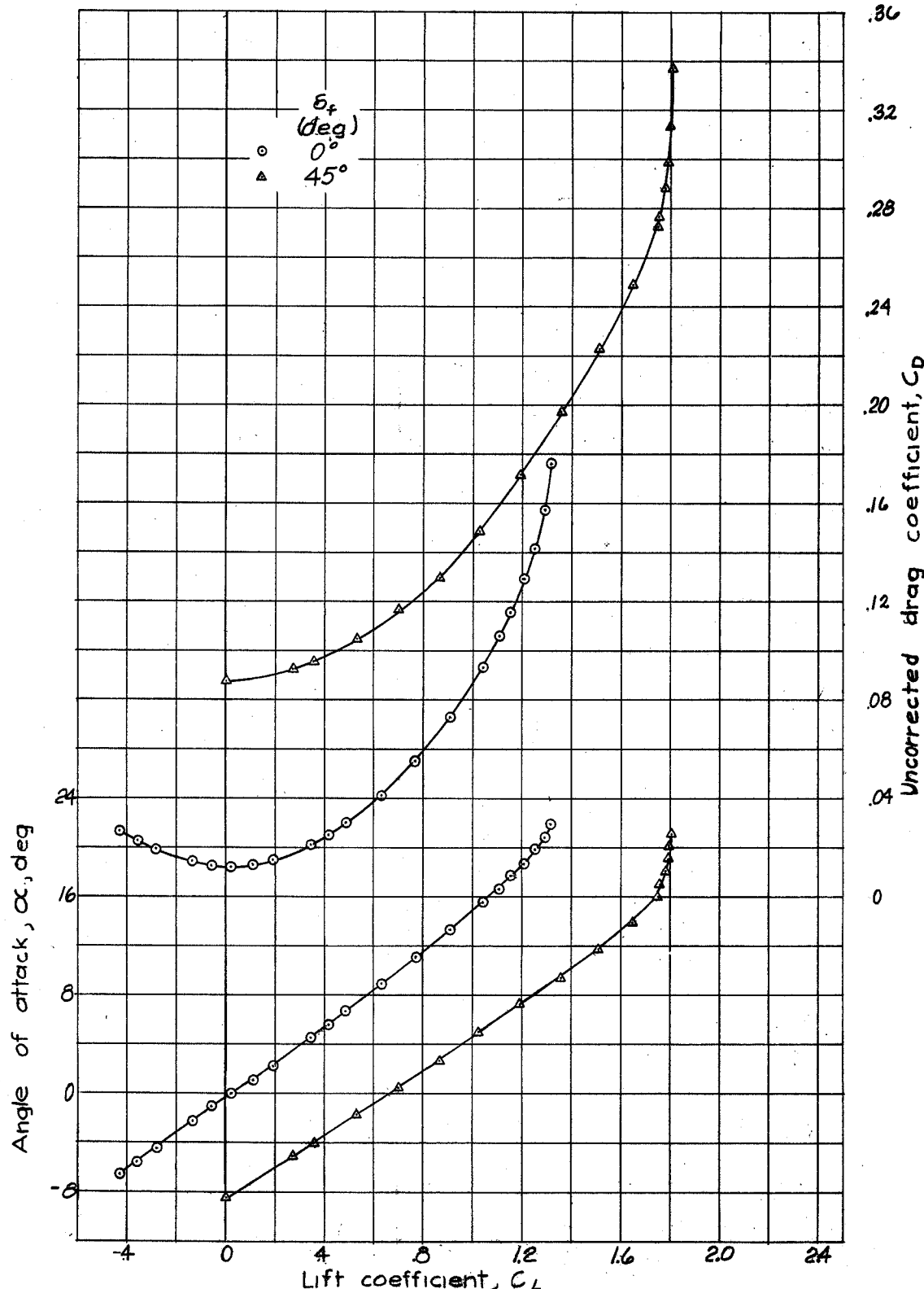


Figure 5.- Lift and drag coefficients of 0.36 scale model of Curtiss XP-60 wing; not corrected for effects of support strut or inboard end treatment.

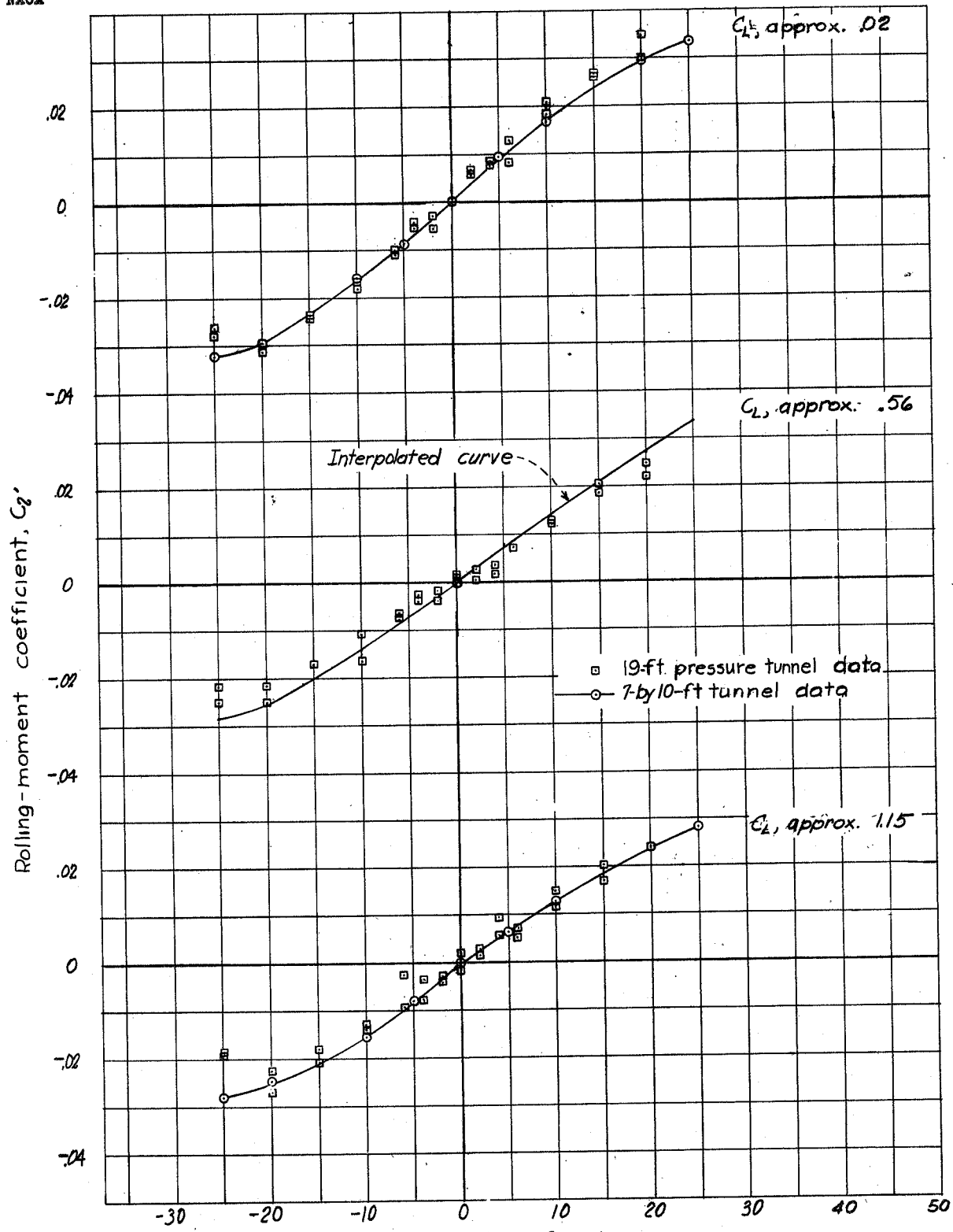


Figure 6.- Characteristics of left aileron with 0.438 cu. balance;  $b_a$ , 36.75 inches. Results from 7-by 10-and 19-foot tunnels; aileron not sealed at ends; 0.36-scale model of Curtiss XP-60 wing.  $\delta_f = 0^\circ$ .

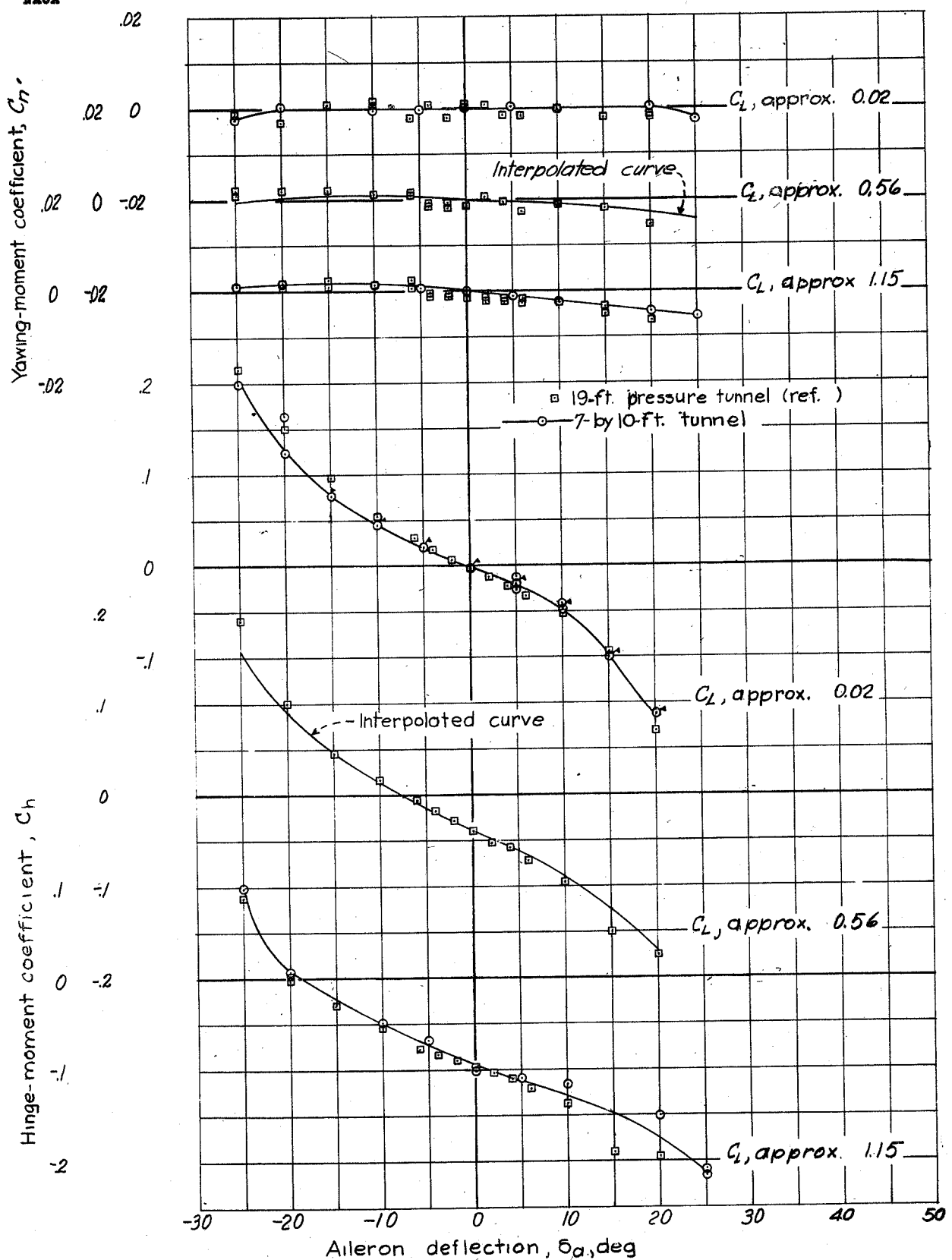
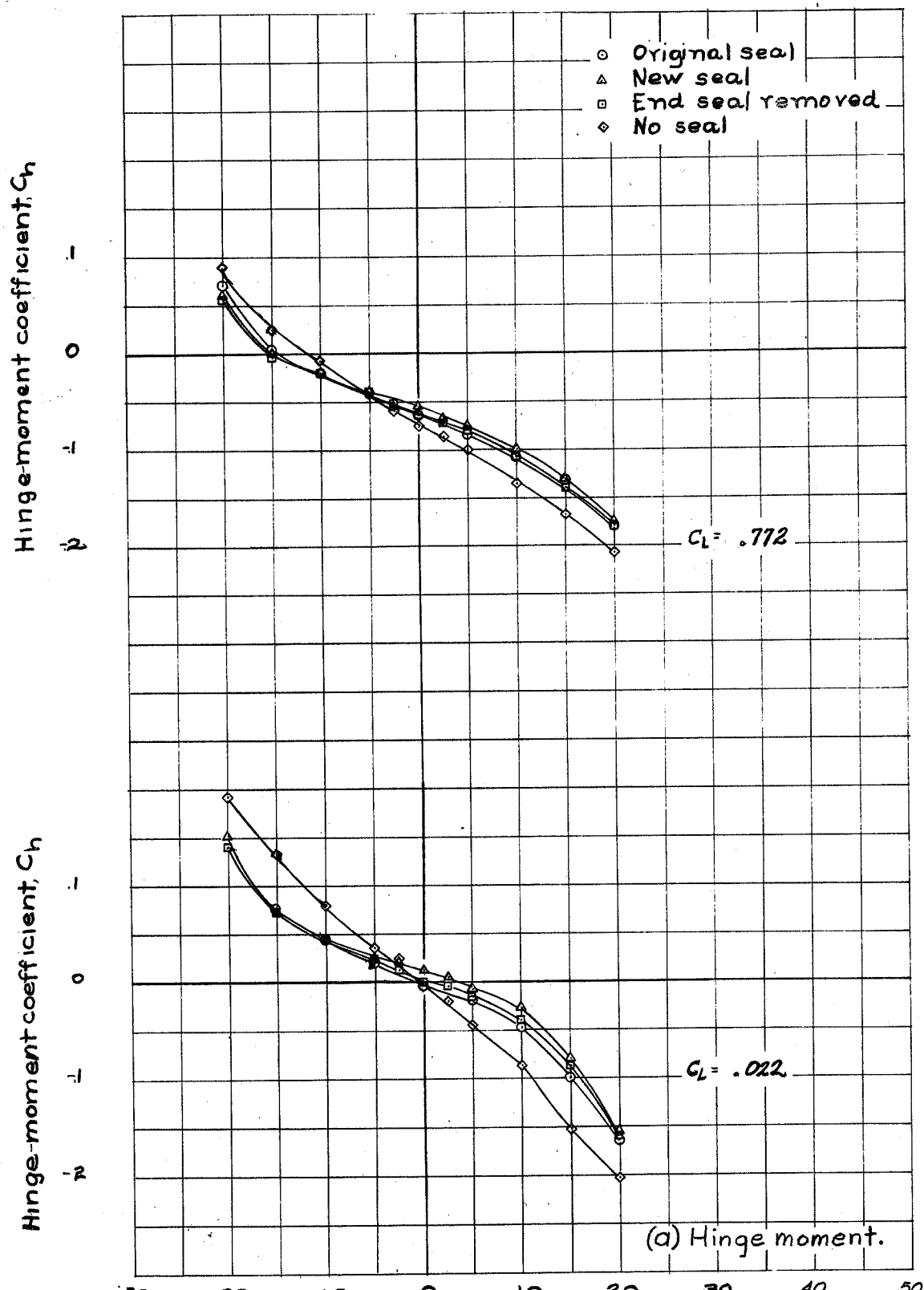


Figure 6 - Concluded.



(a) Hinge moment.

Figure 7.- Characteristics of left aileron with  $0.438 c_a$  balance;  $b_a, 36.75$  inches. Effect of leakage on  $C_h$  and  $C_l$ ; 0.36 scale model of Curtiss XP-60 wing.  $\delta_f = 0^\circ$

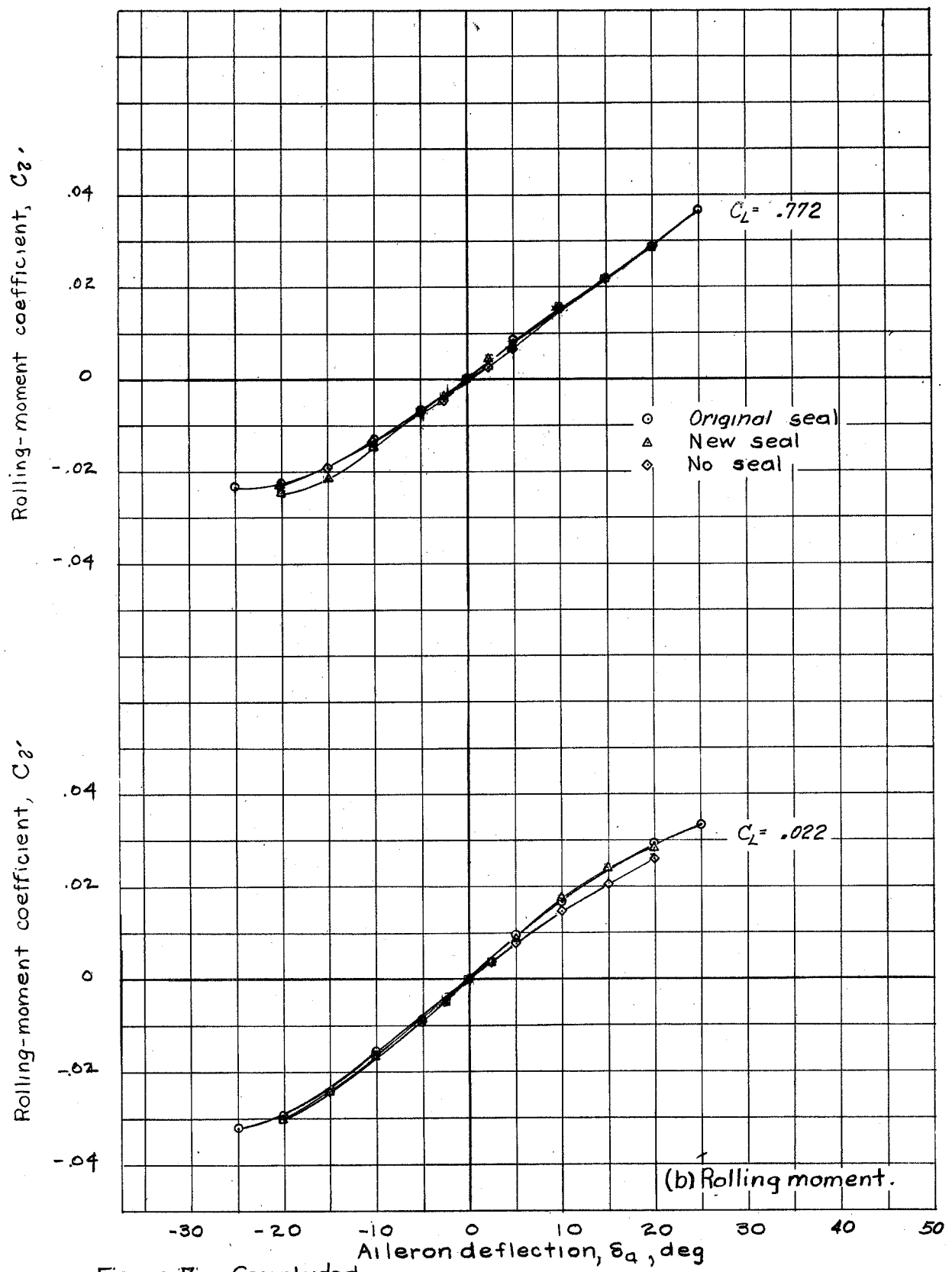


Figure 7. - Concluded.

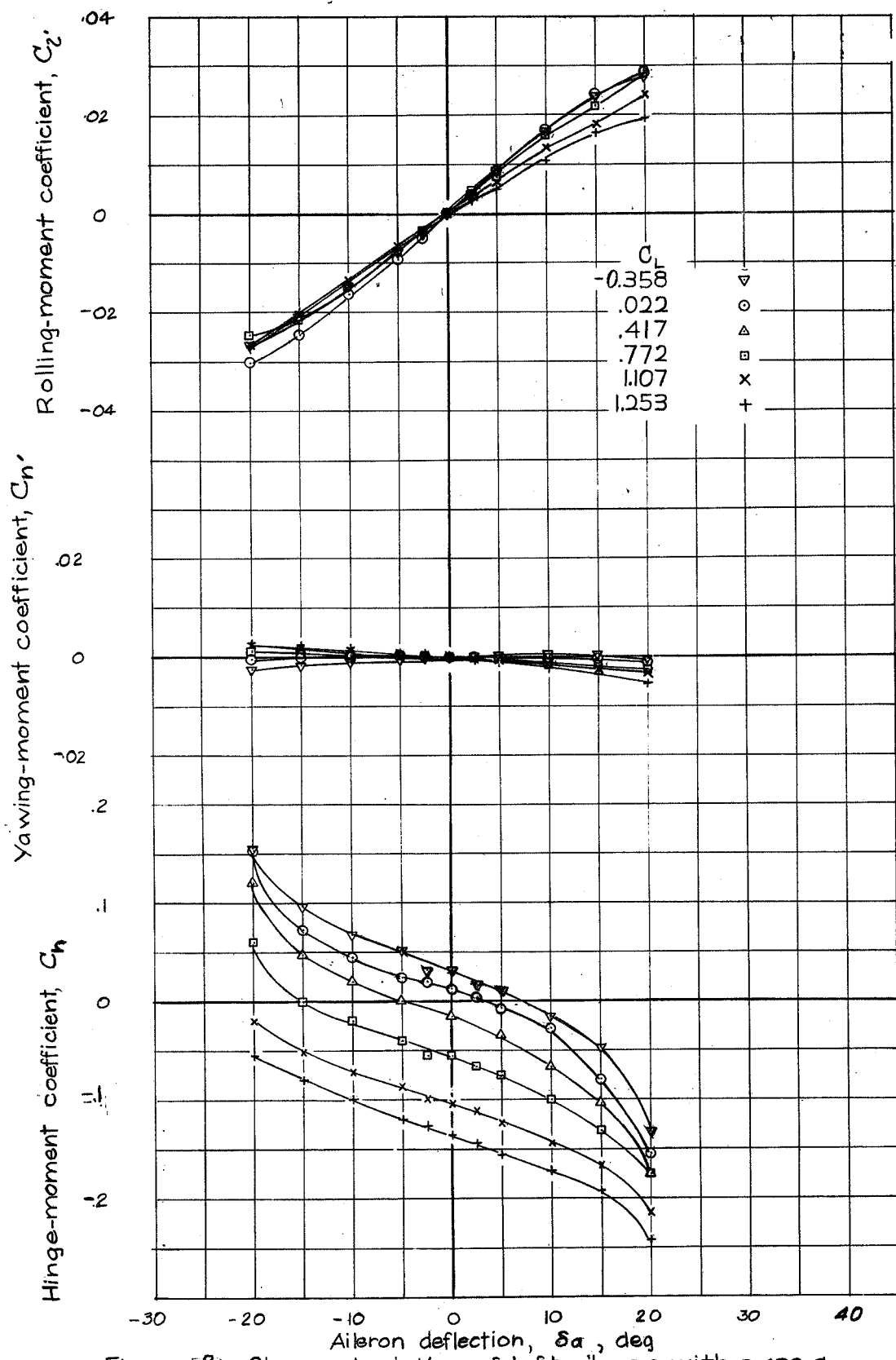


Figure 8.- Characteristics of left aileron with  $0.438 C_a$  balance;  $b_a = 36.75$  inches. Characteristics of aileron with nose and ends of balance sealed; 0.36-scale model of Curtiss XP-60 wing.  $\delta_f = 0^\circ$

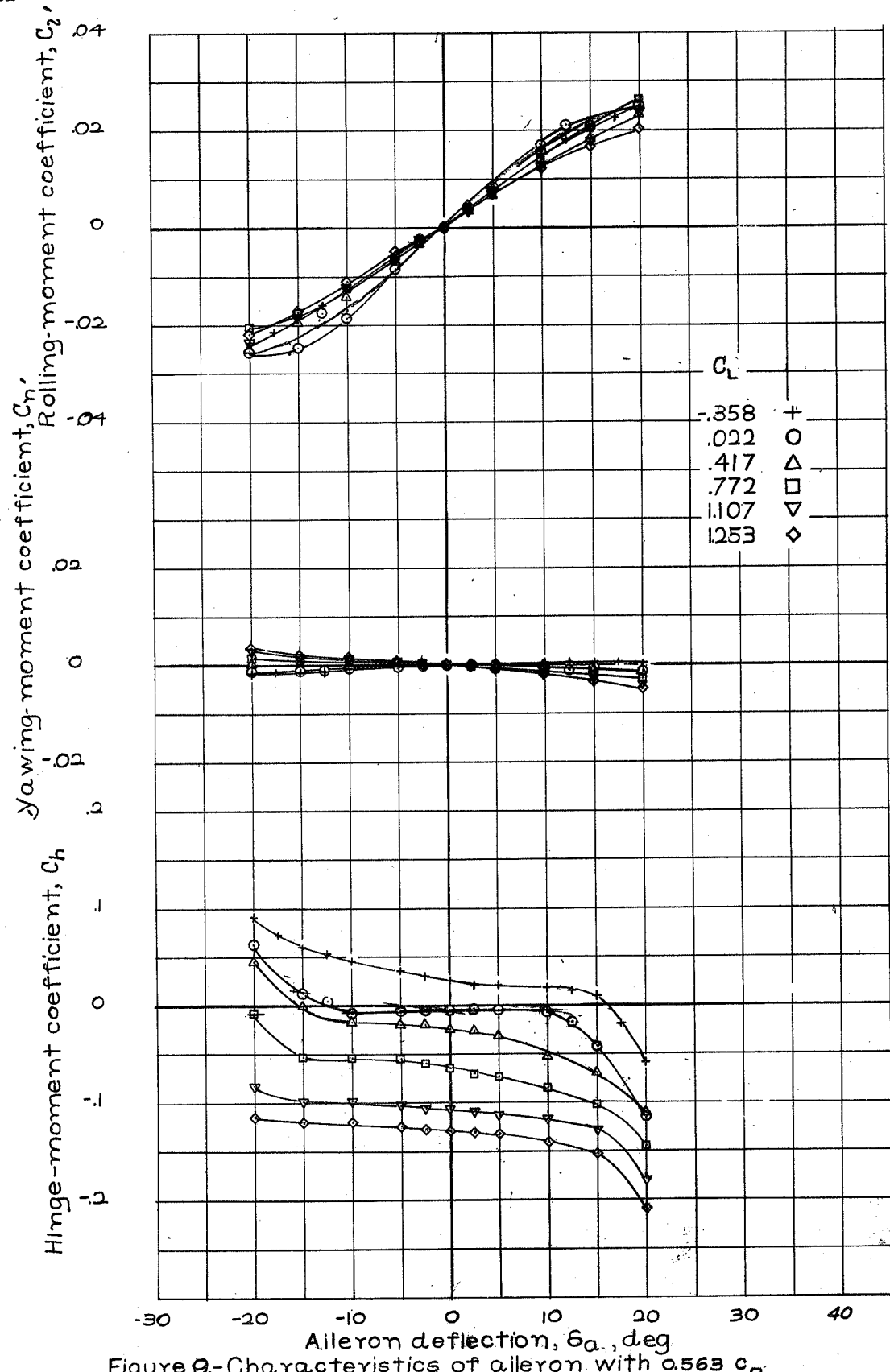


Figure 9.-Characteristics of aileron with  $0.563 c_\alpha$  balance;  $b_\alpha$ , 36.75 inches; 0.36-scale model of Curtiss XP-60 wing.  $\delta_f = 0^\circ$

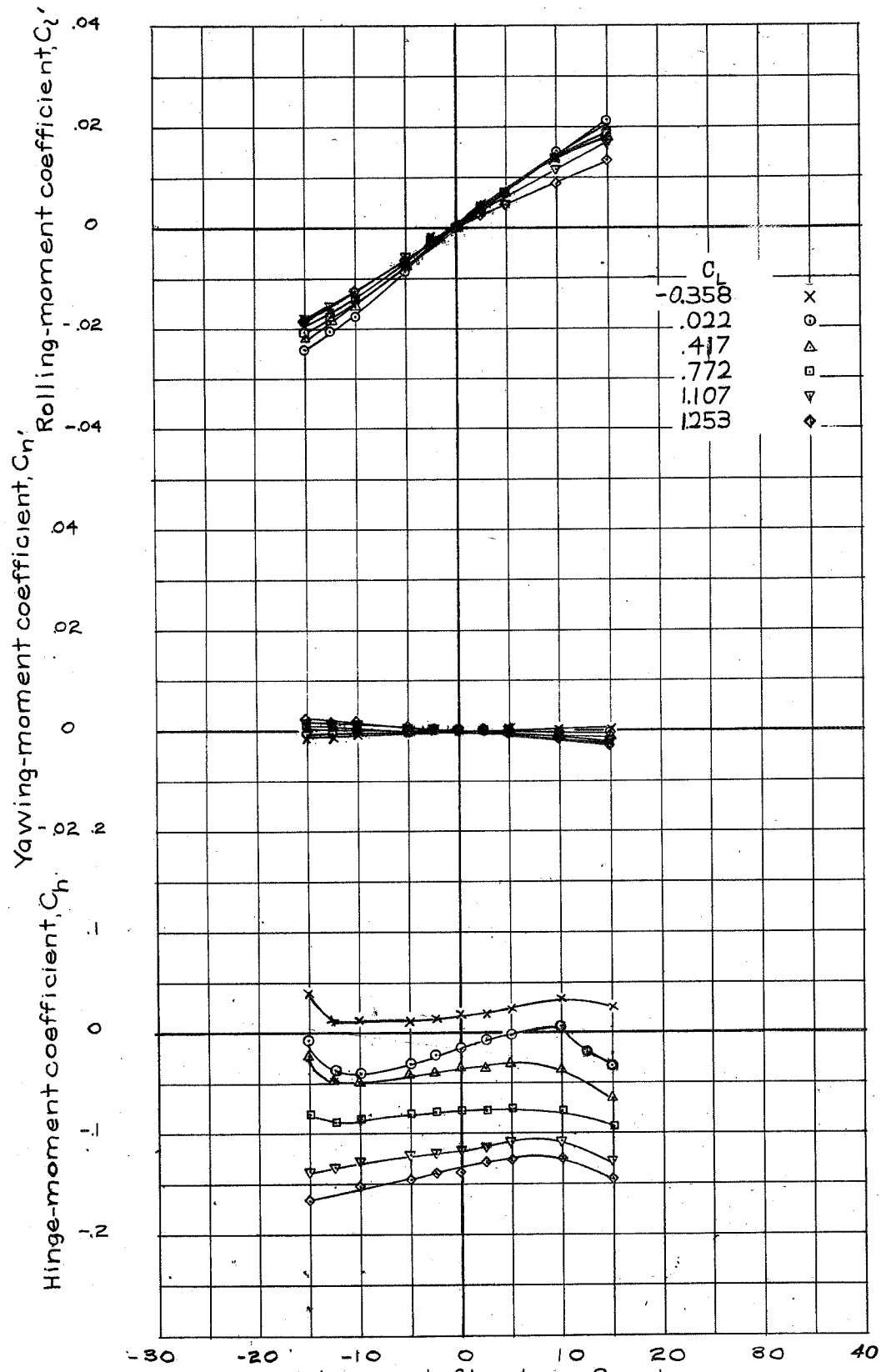


Figure 10.—Characteristics of aileron with  $0.688 c_a$  balance;  $b_a$ , 36.75 inches. Tab neutral; 0.36-scale model of Curtiss XP-60 wing.  $\delta_f = 0^\circ$ .

NACA

Fig. 11a

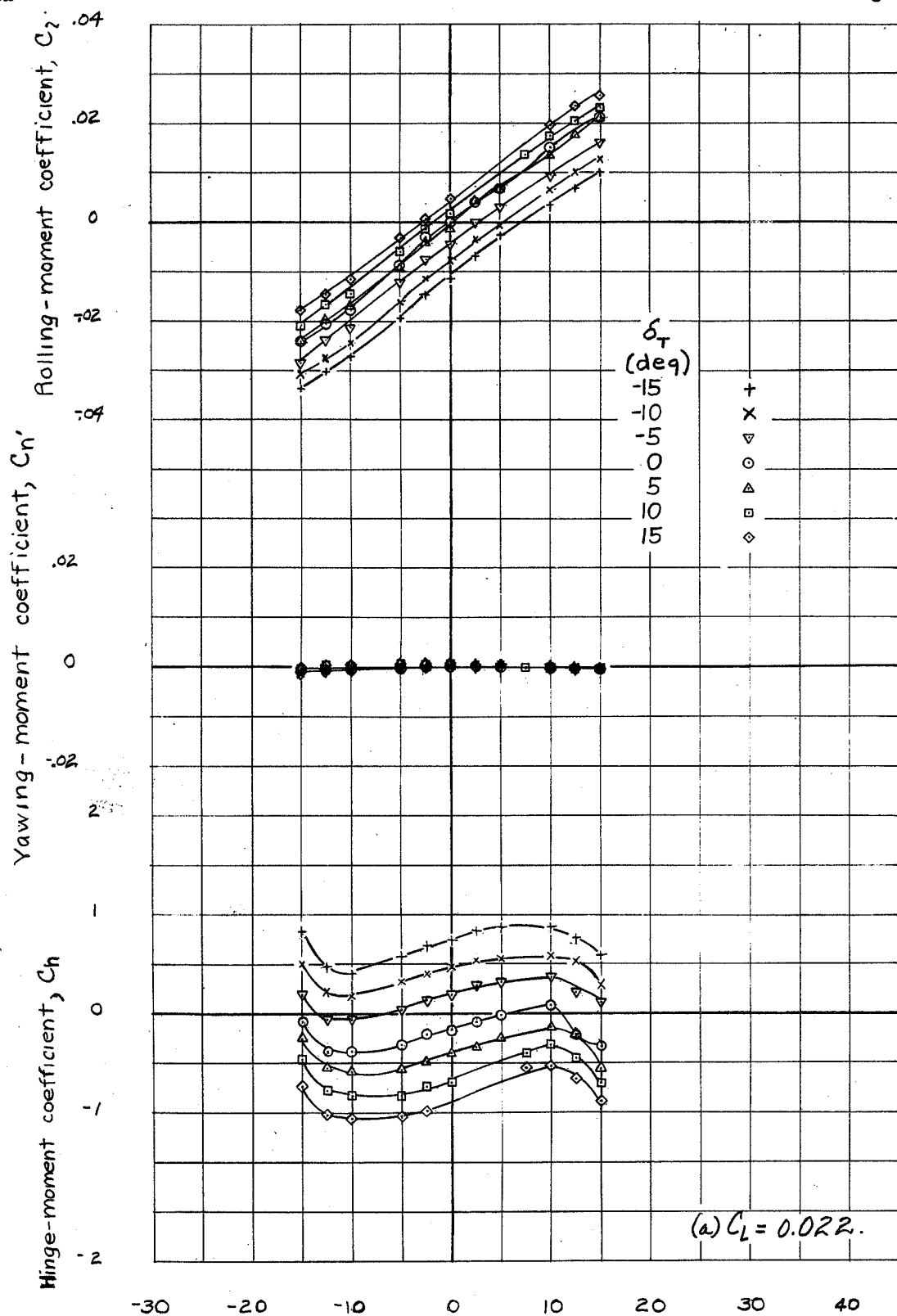


Figure 11.- Characteristics of aileron with 0.688  $c_a$   
 balance;  $b_a$ , 36.75 inches. 0.26  $c_a$  tab deflected along  
 full aileron span; 0.36 scale model of Curtiss XP-60 wing.  
 $\delta_f = 0^\circ$

Fig. 11b

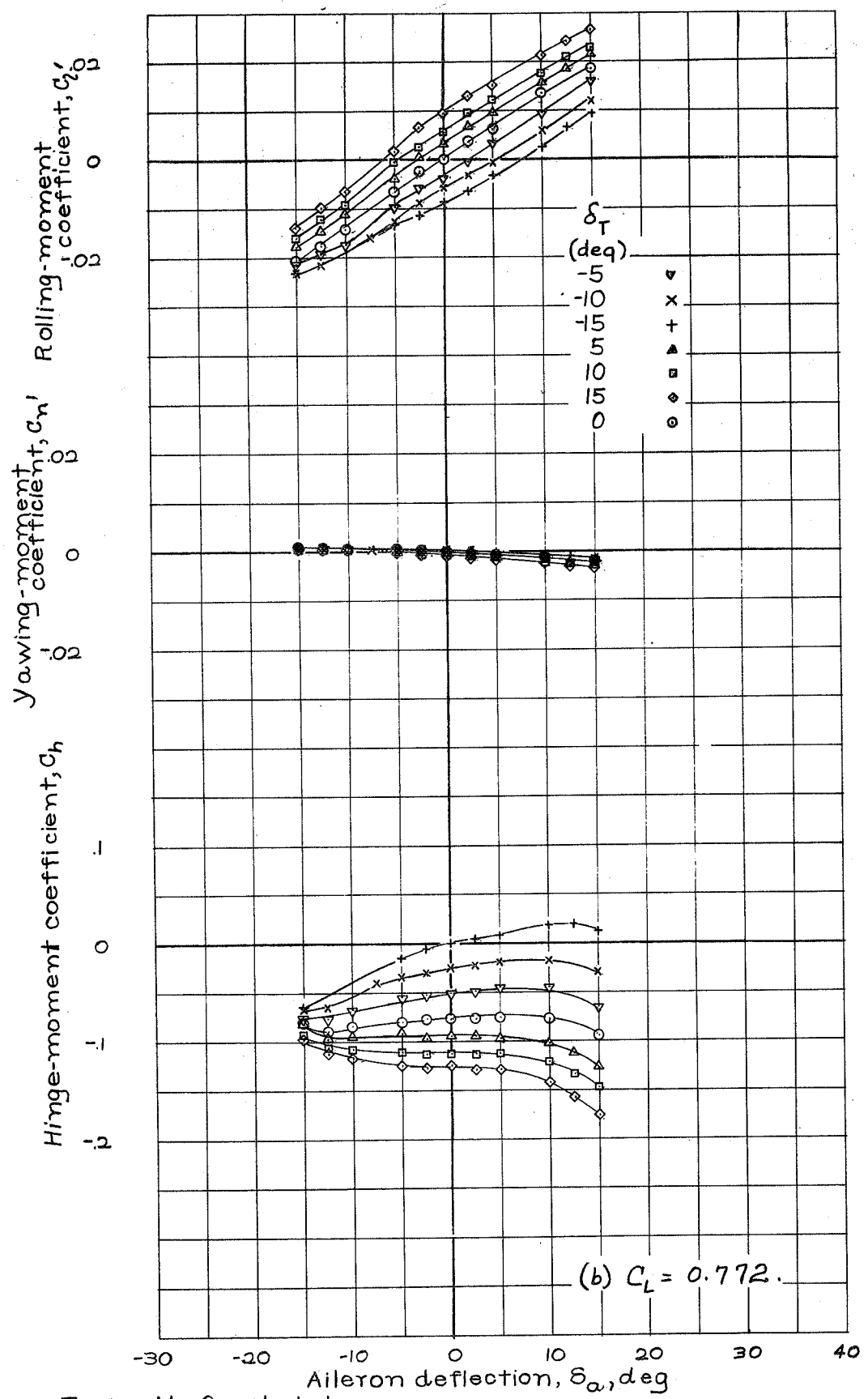


Figure 11.-Concluded.

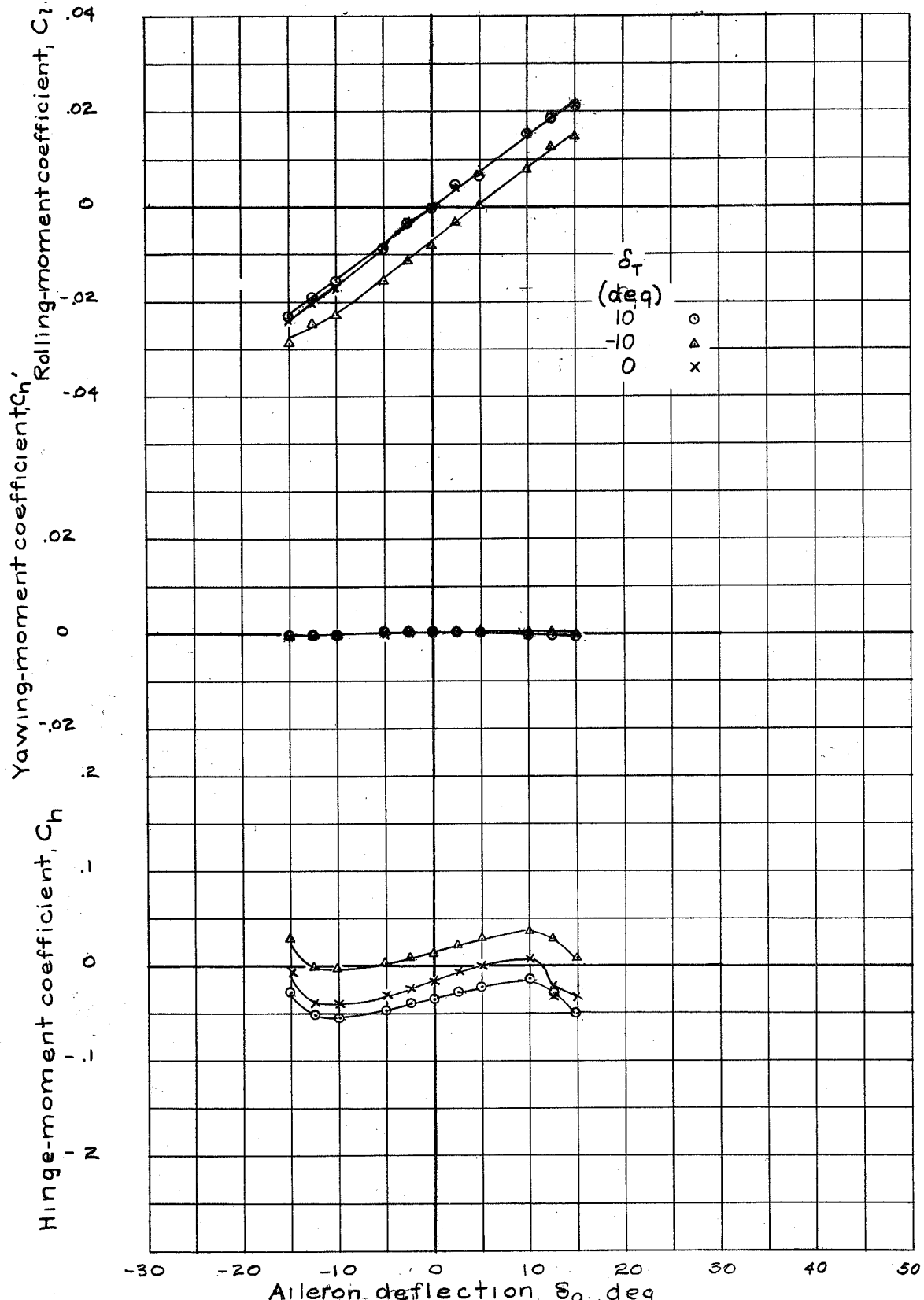


Figure 12.-Characteristics of aileron with 0.688  $C_L$  balance;  $b_{\alpha}$ , 36.75 inches. 0.26  $C_L$  tab deflected along half aileron span; 0.36 scale model of Curtiss XP-60 wing;  $C_L = .022$ .  $\sigma_f = 0^\circ$ .

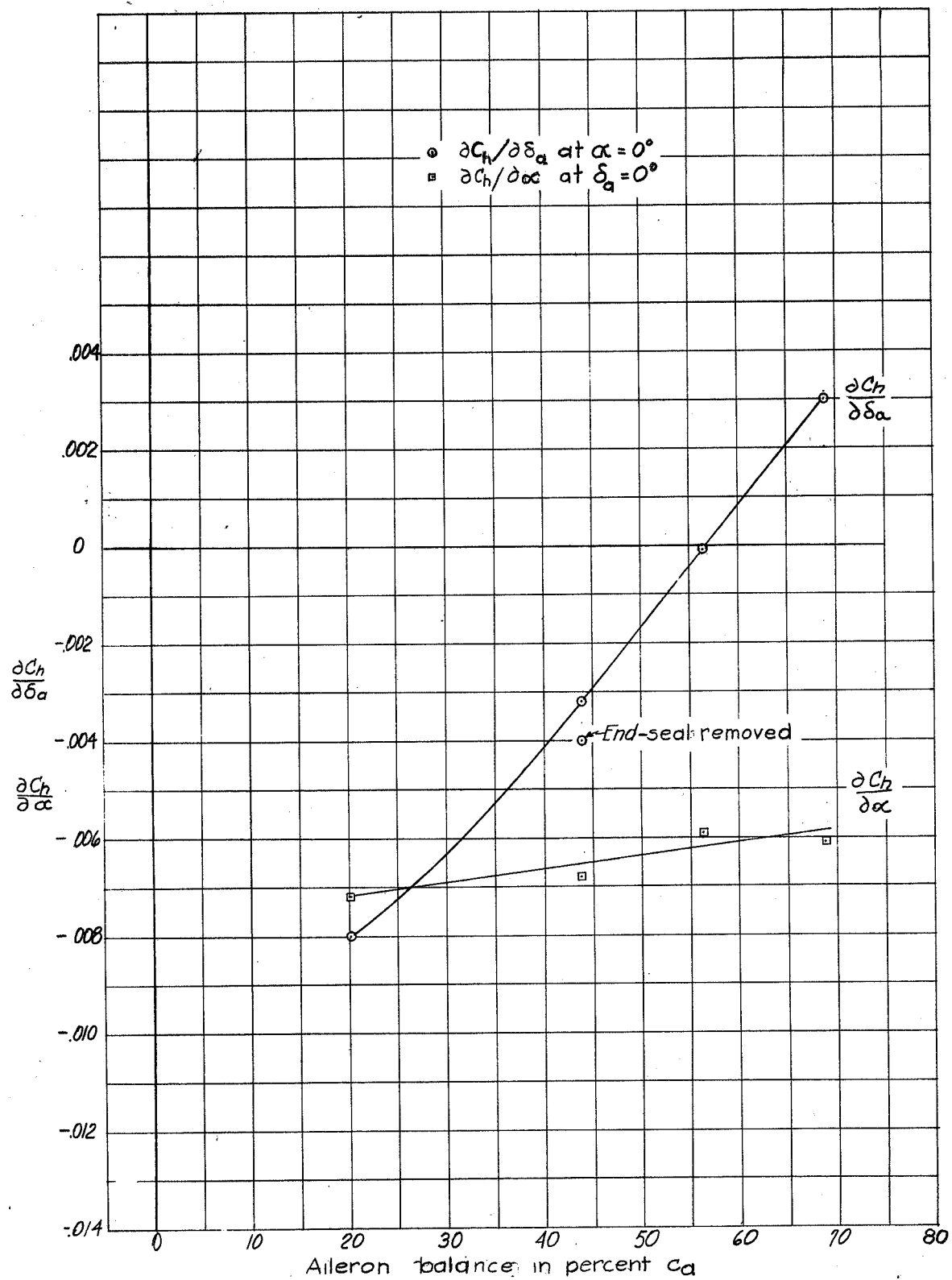


Figure 13.—Effect of balance upon slopes of hinge-moment coefficient curves,  $\frac{\partial C_h}{\partial \delta_a}$  and  $\frac{\partial C_h}{\partial \alpha}$ ; 0.36 scale model of Curtiss XP-60 wing.  $\delta_f = 0^\circ$ .

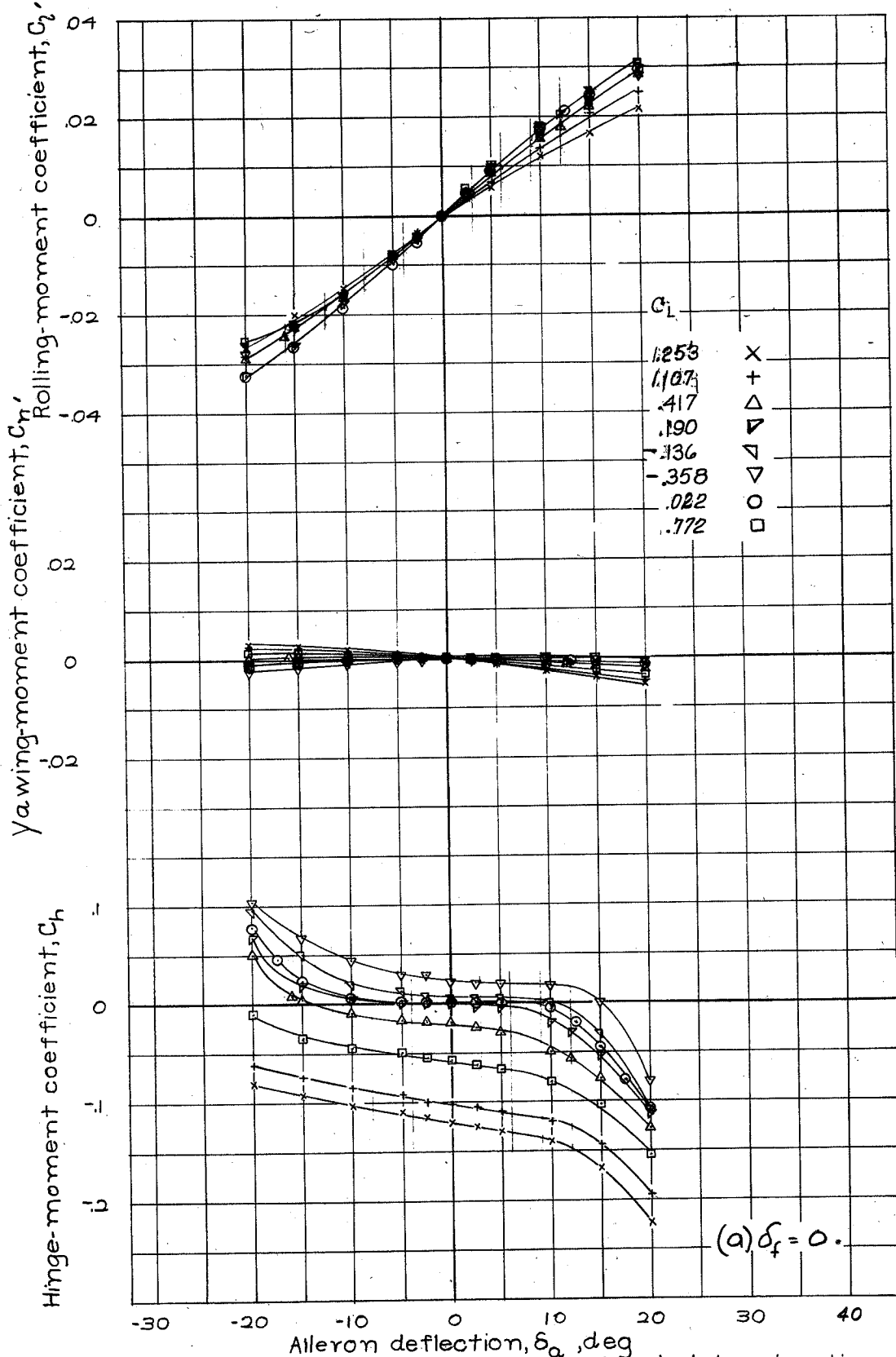


Figure 14.-Characteristics of aileron extended to wing tip; balance,  $0.563 c_a$  extending outboard from midspan of original aileron; tab neutral; 0.36 scale model of Curtiss XP-60 wing.

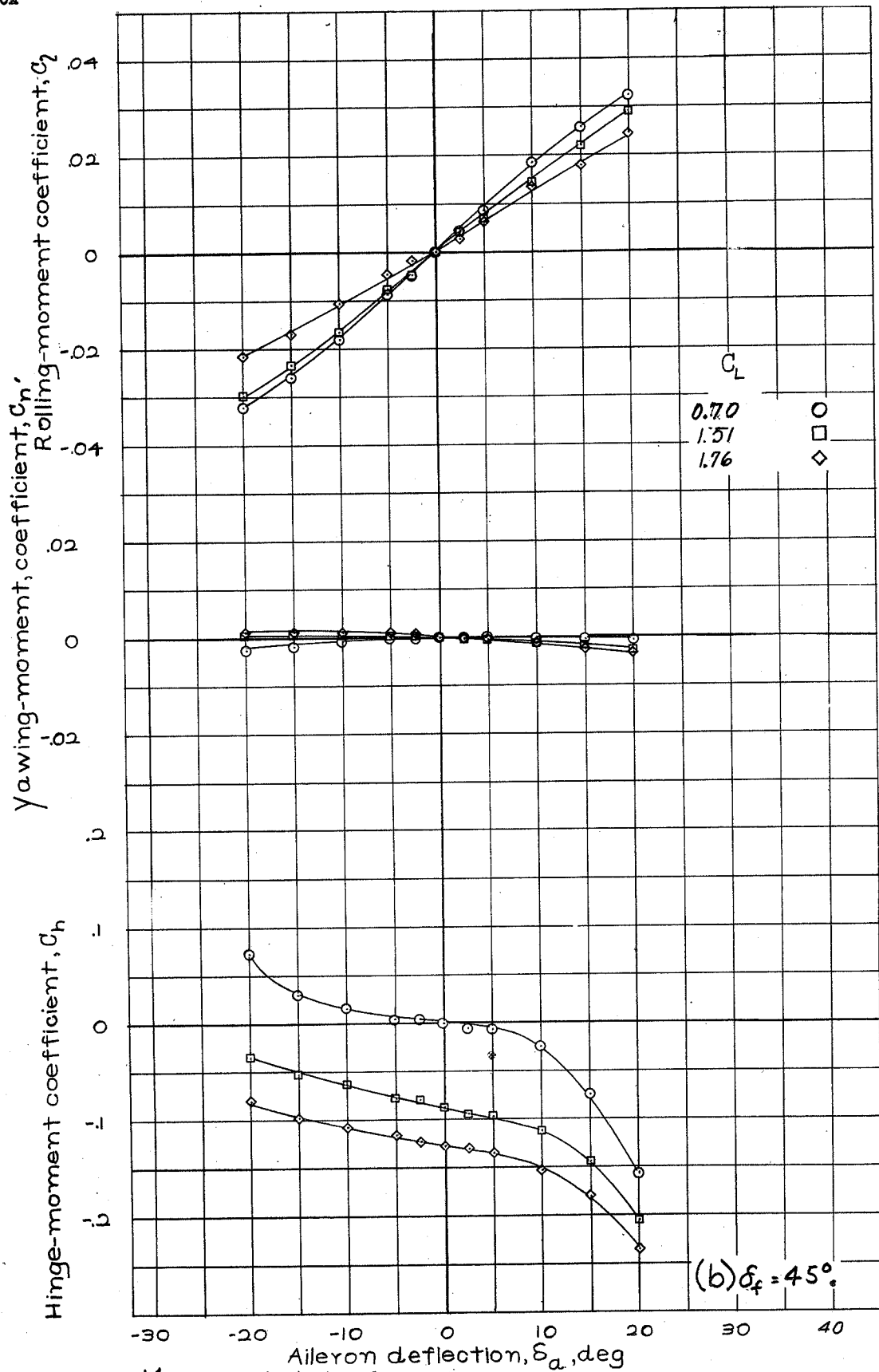


Figure 14.—Concluded.

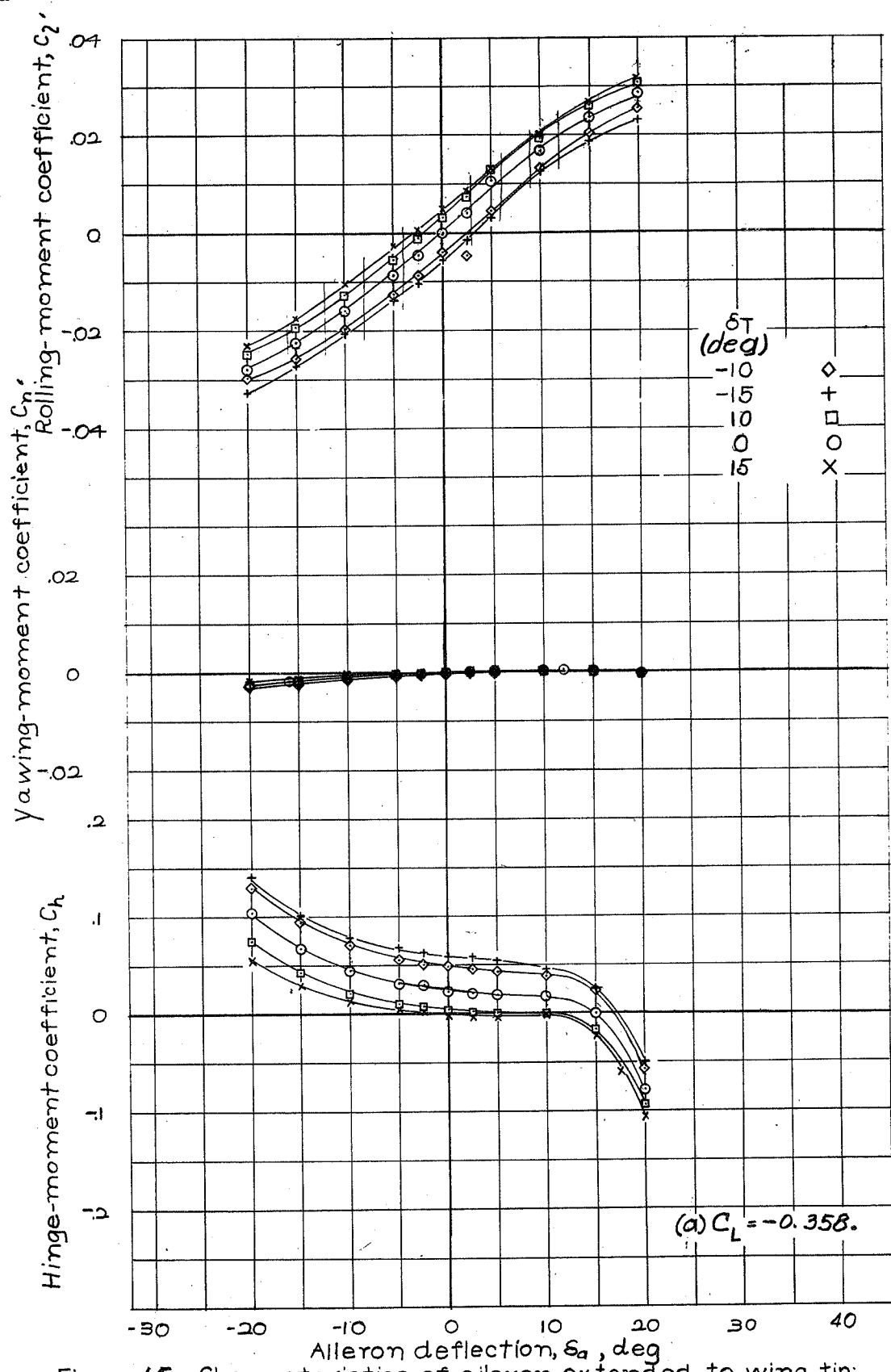


Figure 15.- Characteristics of aileron extended to wing tip; balance, 0.563  $c_{\bar{A}}$ ; tab 0.26  $c_{\bar{A}}$  extending outward from midspan of original aileron; tab deflected;  $\delta_T = 0^\circ$ ; 0.36-scale model of Curtiss XP-60 wing.

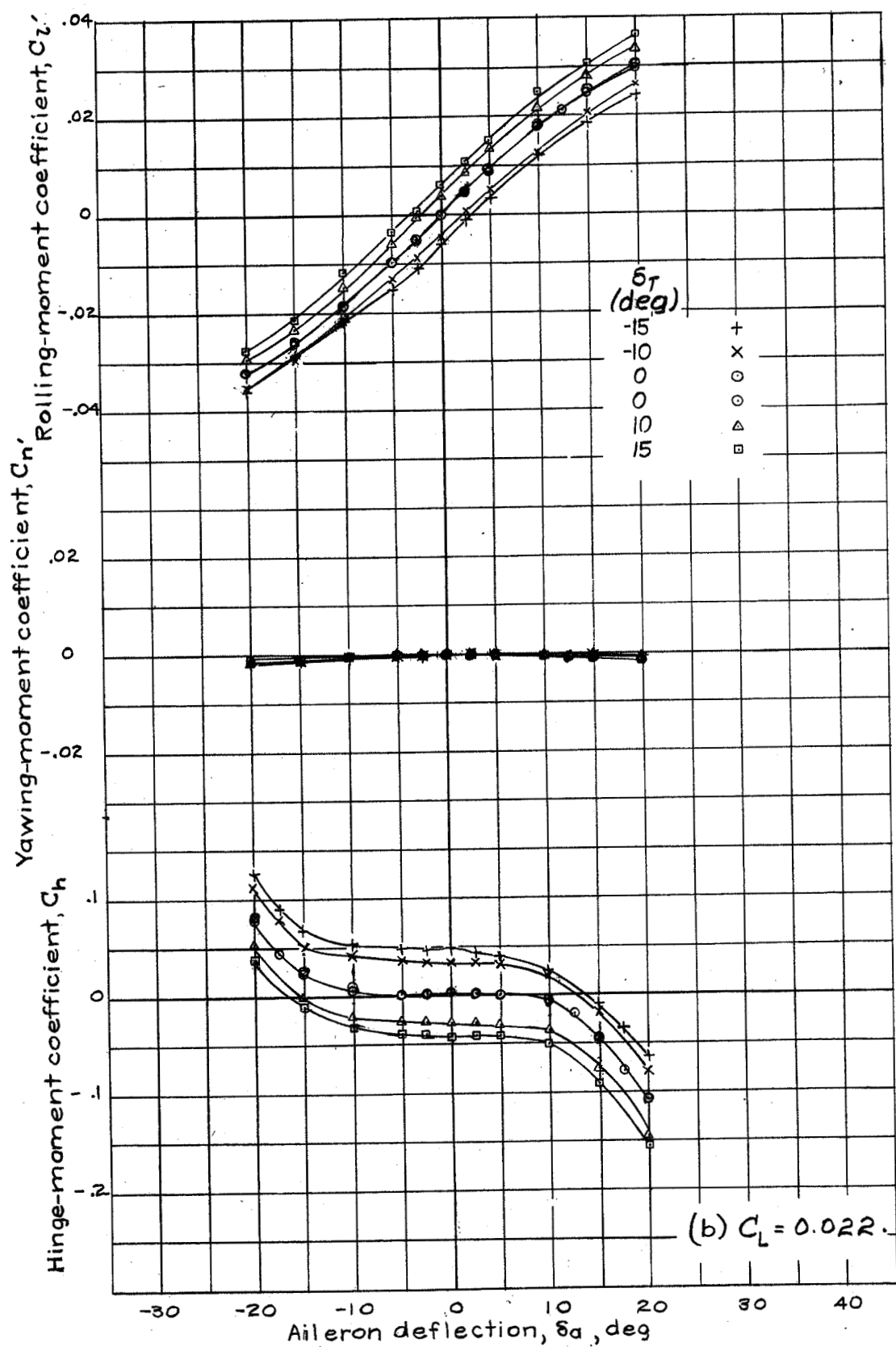


Figure 15.-Continued.

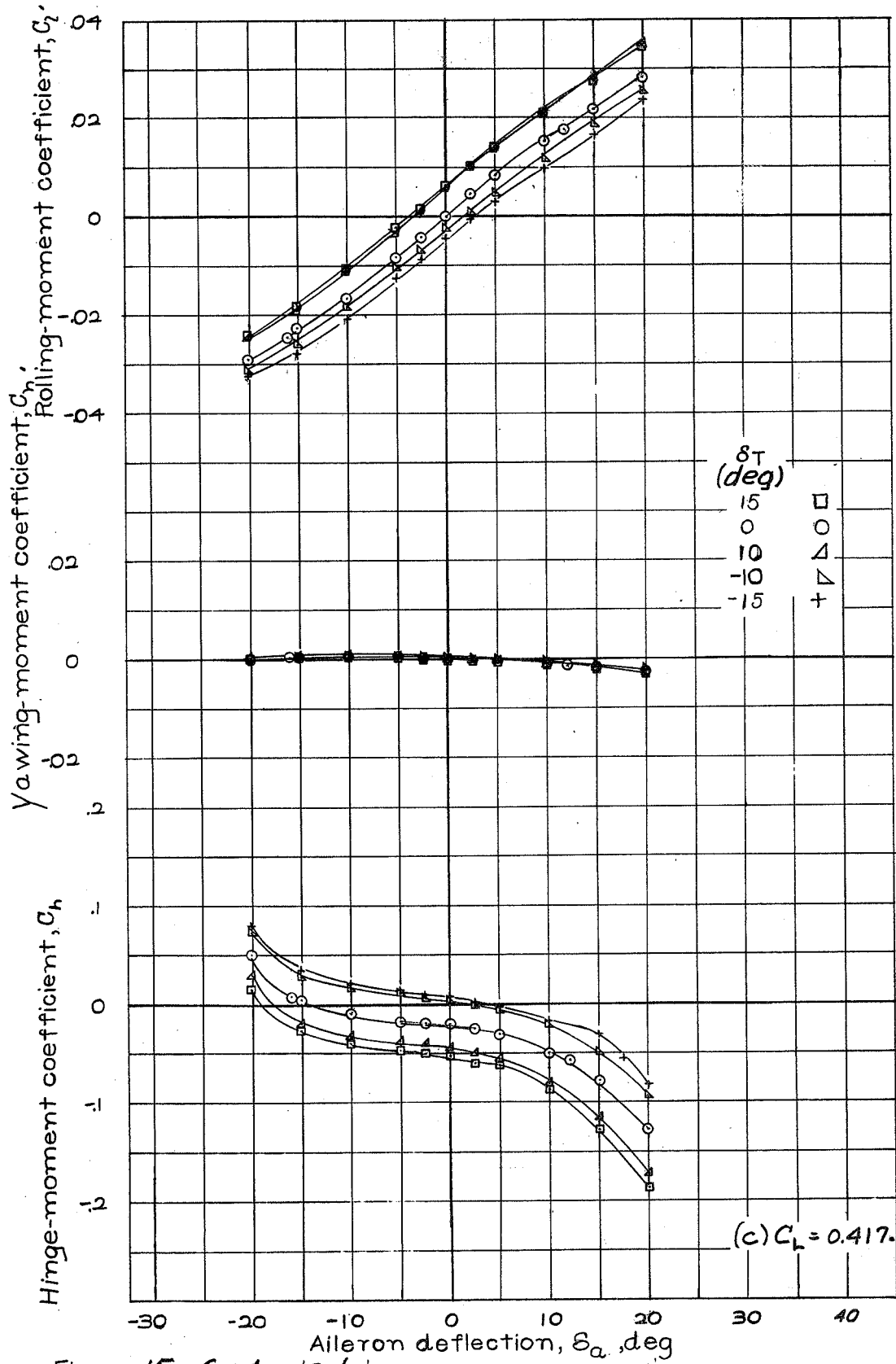


Figure 15.-Continued.

Fig. 15d

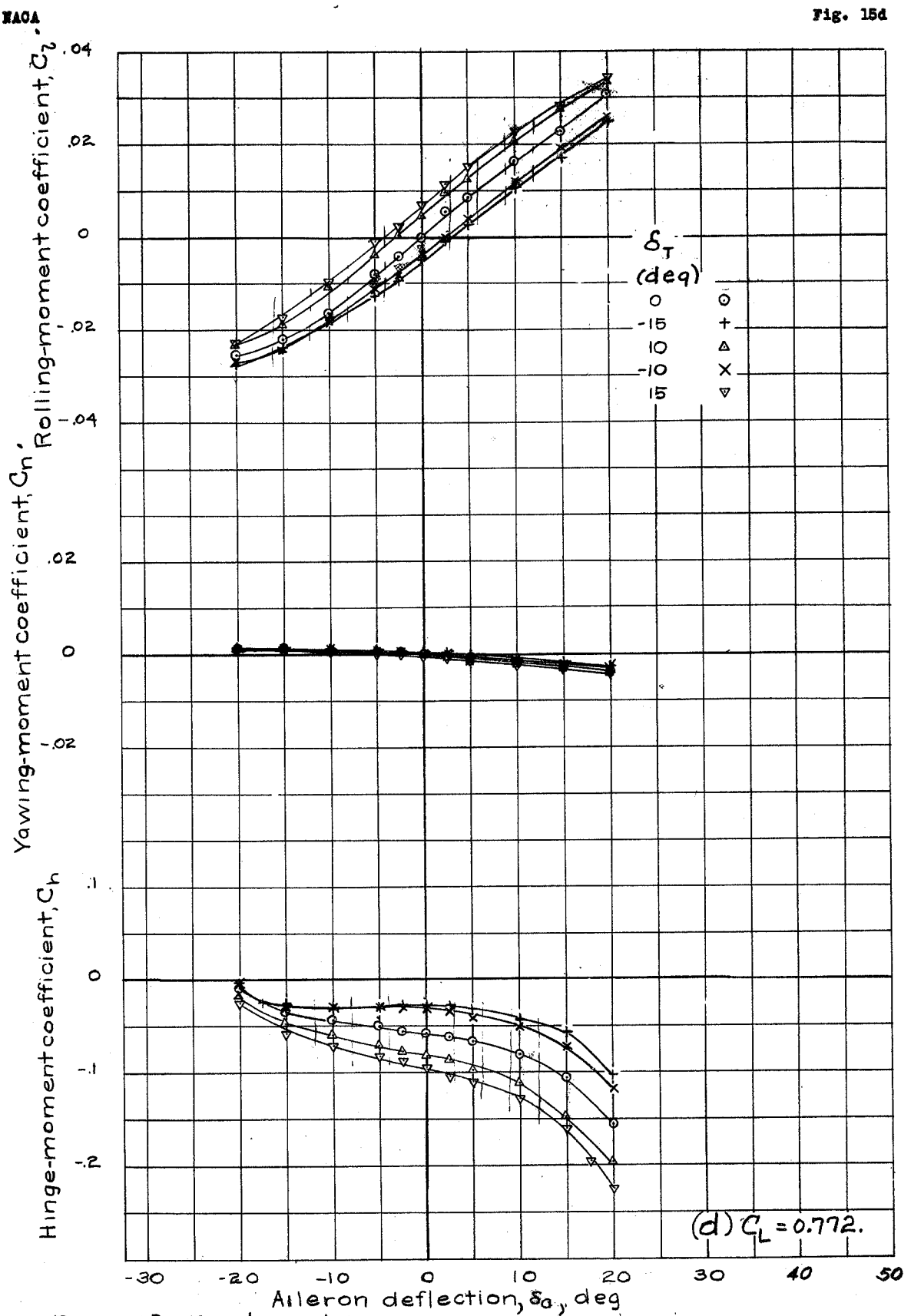


Figure 15.-Continued.

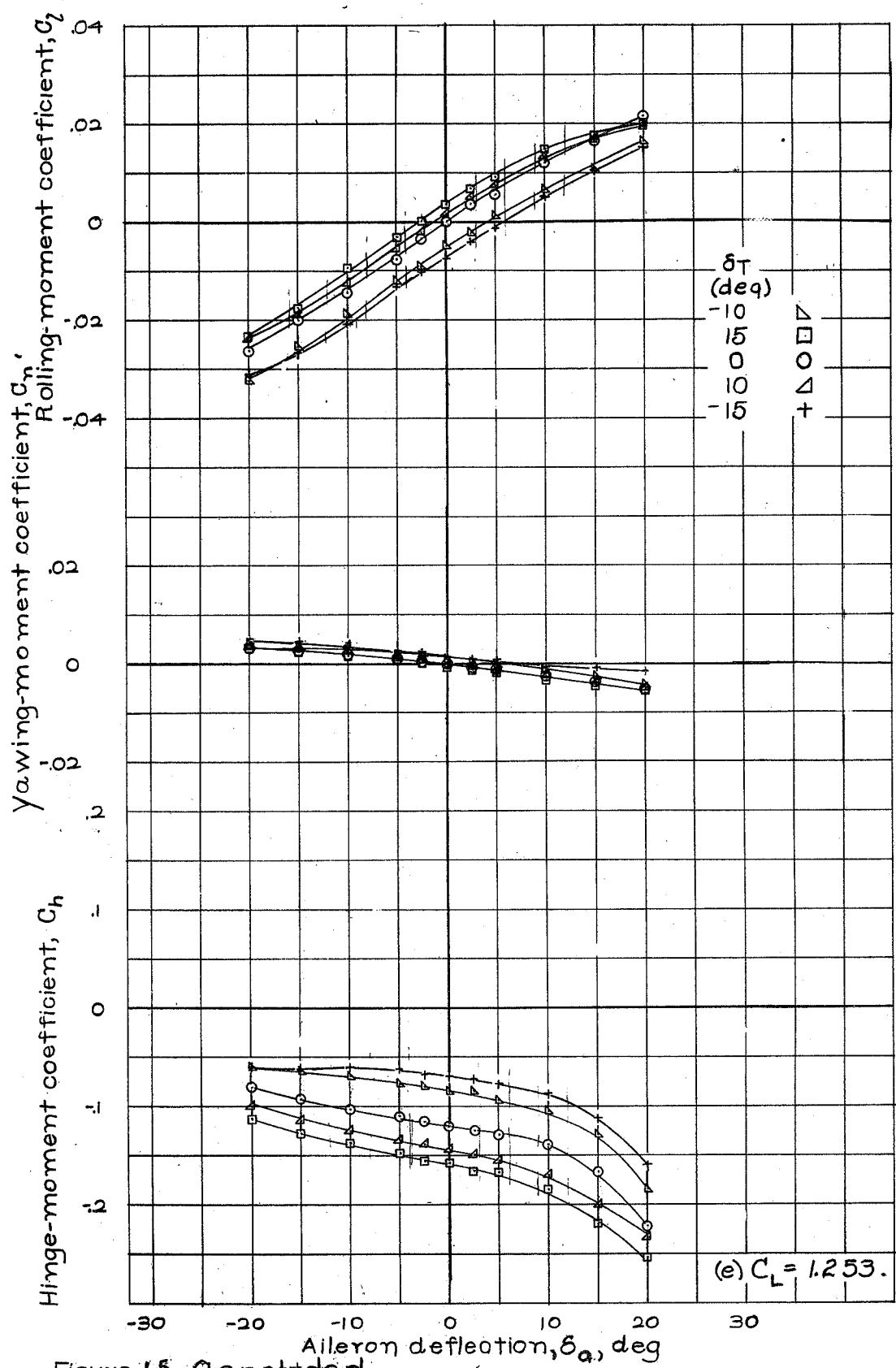


Figure 15.-Concluded.

FIGURE 16

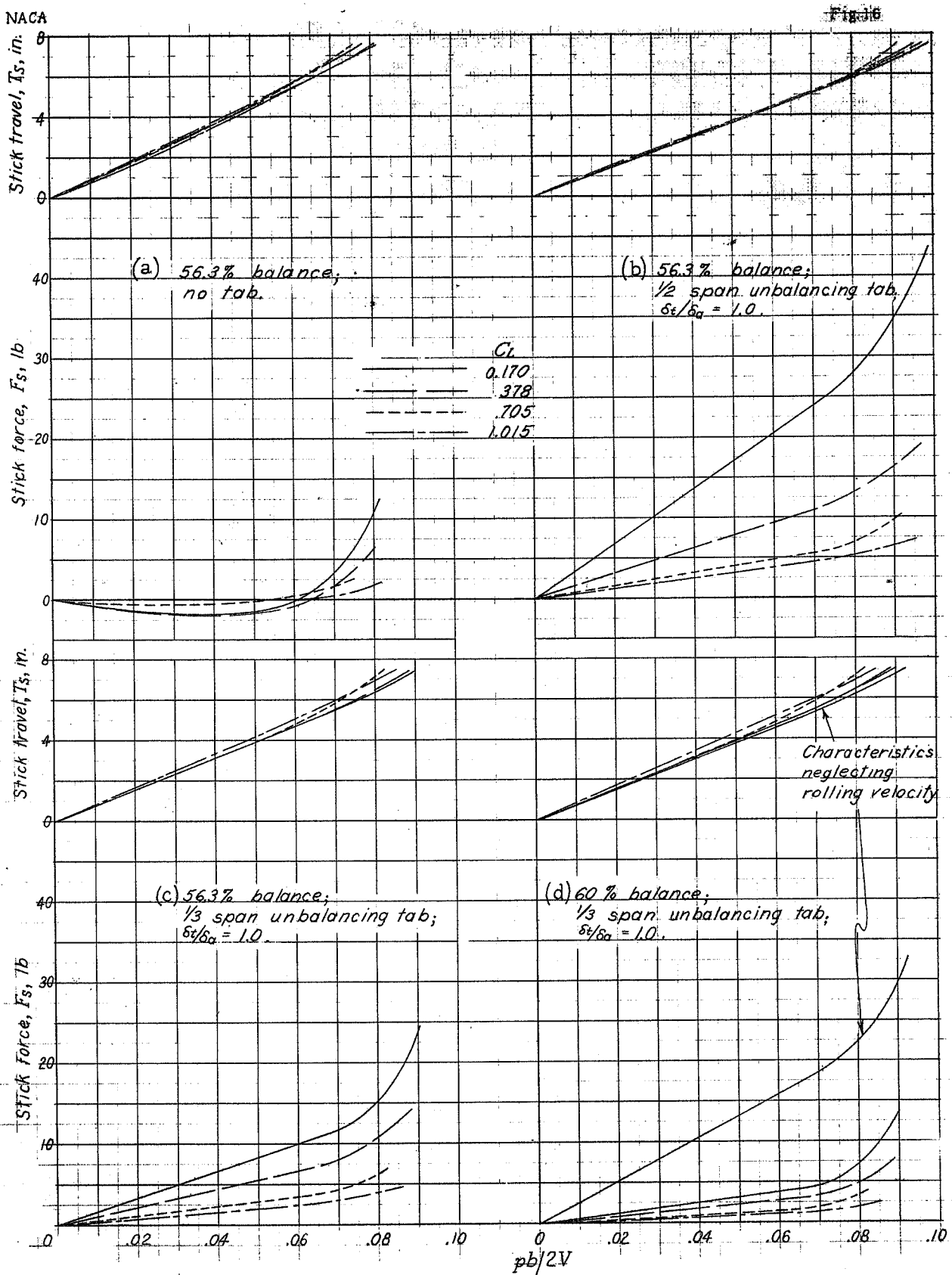


Figure 16. Aileron control characteristics of the XP-60 airplane.